Joint master of Mediterranean Initiatives on renewable and sustainable energy		

Palestine Polytechnic University

Deanship of Graduate Studies and Scientific Research

Master Program of Renewable Energy and Sustainability

Controlling of Multi-Level Inverter Under Shading Conditions Using Artificial Neural Network.

By

Abdulsami.A.A.Qawasmi

Supervisor

Prof. Sameer Khader

Thesis submitted in partial fulfillment of requirements of the degree

Master of Science in Renewable Energy & Sustainability

August , 2019

Joint master of Mediterranean Initiatives on renewable and sustainable energy

The undersigned hereby certify that they have read, examined and recommended to the Deanship of Graduate Studies and Scientific Research at Palestine Polytechnic University and the Faculty of Science at Al-Quds University the approval of a thesis entitled:

Controlling of Multi-Level Inverter Under Shading Conditions Using Artificial Neural Network.

Submitted by
Abdulsami.A.A.Qawasmi

In partial fulfillment of the requirements for the degree of Master in Renewable Energy & sustainability.
Graduate Advisory Committee:
Prof. Sameer Khader ……………………………….,…………………………..
(Supervisor), University (typed)
Date: ______________ Signature:______________

Prof./ Dr. ……………………………., …………………………………..
(Co-supervisor), University (typed)
Date: ______________ Signature:______________

Prof. Abdel Karim Dauod…………………………………………,……………………..
(Internal committee member), University (typed).
Date: ______________ Signature:______________

Dr.Mahran Quran. ……………………………………………,……………………..
(External committee member), University (typed).
Date: ______________ Signature:______________

Thesis Approved by:

Name: Dr.Murad Abu Subeih

Dean of Graduate Studies & Scientific Research

Palestine Polytechnic University

Signature:…………………………………….

Date:…………………………………….

Controlling of Multi-Level Inverter Under Shading Conditions Using Artificial Neural Network.

By **Abdulsami.A.A.Qawasmi**

ABSTRACT

In real life the PV sources can't supply multilevel inverters with equal and constant DC voltage. The variation of irradiation affects the output voltage of PV's which in turn vary the switching angles required to switch Multi level Inverter MLI to achieve minimum contents of output voltage profile , so the harmonic elimination's equations must be solved for each set of input DC voltages. This research present how can we use genetic algorithm (GA) to solve harmonic elimination equations of 11 level CHB inverter with equal and non-equal DC sources , then artificial neural network (ANN) is used to switch CHB with suitable angles for any set of input DC sources .

The partial shading of PV modules from clouds, obstacles are responsible for unequal DC supply for multilevel inverter.

A set of mathematical equations representing the general output waveform of the multilevel inverter with non-equal DC sources is formulated using Fourier series, then GA is used to solve the none linear equations to get the optimal set of switching angles which minimize the total harmonic distortion (THD) of eleven level inverter to acceptable limit, after that ANN is trained to generate these angles in any case of DC voltage variation in short time including constant DC sources when no shading

FFT analyses are carried out for output voltage profile to prove that this technique is reliable for MLI; the proposed technique is validated through simulation by matlab Simulink Ra2013.

GA and ANN technique achieve minimum THD for both equal and unequal DC sources, and can be applied for any kind of level inverter. According to calculations it is found that THD for equal DC sources was 9.38%, and for variable DC sources was 10.26% when input DC maximum variation was 4.47 volts, and 12.93% when input DC maximum variation was 11.43 volts.

The results showed the effectiveness of GA in solving mathematical equations and the effectiveness of the neural network in giving excellent results that reach 99% of the real values.

دراسة استخدام الشبكة العصبونية للتحكم في Multi-Level Inverter عند وجود الظل

اعداد: عبدالسميع عبدالفتاح القواسمة

ملخص

اصبح ربط مزارع الخلايا الشمسية بشبكة الكهرباء لغة العصر، ولكن المشكلة تكمن في تحويل مصادر الجهد والتيار الثابتين (DC Sources) الى موجات جيبية (Sine Wave) لتتوافق مع موجة الكهرباء الجيبية، لقد تم استخدام انواع مختلفة من العاكسات (Inverters) لكل نوع حسناته وسيئاته ومعظمها يعتمد عاى ان مصادر فرق الجهد ثابتة، ولكن في حالة وجود الظل يصبح ناتج هذه العاكسات محملا ب (Harmonics) التي تؤذي الاحمال المربوطة بالشبكة ولعلاج هذه المشكلة تم استخدام انواع الفلاتر المختلفة للحد من هذه الظاهرة

في هذا البحث تم دراسة استخدام عاكس متعدد المستويات (Multi-Level Inverter) كاحد الانواع التي يمكنها من تقليل ظاهرة الهارمونيك على الشبكة عن طريق قدح الترانزستورات (IGBTs) بزوايا مناسبة سواء كانت مصادر الجهد ثابتة ام متغيرة

لقد تم استخدام جينيتيك الجوريثم (Genetic Algorithm) لحل المعادلات الغير خطية المرتبطة بايجاد افضل زوايا القدح ، ثم تم تدريب الشبكة العصبونية على النتائج التي حصلنا عليها من GA لتستطيع توليد زوايا القدح مهما تغيرت مصادر الجهد في حالة وجود ظل على الخلايا الشمسية

تم استخدام برنامج Matlab Ra2013 لكتابة برنامج GA وتدريب الشبكة العنكبوتية و تصميم نموذج محاكاة ربط خمس خلايا شمسية ب (Single Phase Eleven level Inverter)

لقد اظهرت النتائج ان (THD) انخفض الى قيمة 9.3% بدون استخدام الفلاتر في حالة تساوي مصادر الجهد المزودة للعاكس، وارتفعت قيمته من 10.26% عندما اصبحت قيمة التغير في مصادر الجهد نتيجة وجود الظل يساوي 4.47 فولت ووصل الى 12.94% عندما اصبحت قيمة التغير في الجهد يساوي 11.43 فولت

لقد اظهرت النتائج فعالية (GA) في حل المعادلات الرياضية وفعالية الشبكة العصبونية في اعطاء نتاج ممتازة تصل دقتها الى 99% من القيم الحقيقية .

	JAMILA	
Joint master of Mediterranean Initiatives on renewable and sustainable energy		

DECLARATION

I declare that the Master Thesis entitled**" Controlling of Multi-Level Inverter under Shading Conditions Using Artificial Neural Network."** is my own original work, and herby certify that unless stated, all work contained within this thesis is my own independent research and has not been submitted for the award of any other degree at any institution, except where due acknowledgement is made in the text.

Student Name: **Abdulsami.A.A.Qawasmi**

Date: ________________ Signature:________________

Joint master of Mediterranean Initiatives on renewable and sustainable energy		

STATEMENT OF PERMISSION TO USE

In presenting this thesis in partial fulfillment of the requirements for the joint Master's degree in Renewable Energy & Sustainability at Palestine Polytechnic University and Al-Quds University, I agree that the library shall make it available to borrowers under rules of the library.

Brief quotations from this thesis are allowable without special permission, provided that accurate acknowledgement of the source is made.

Permission for extensive quotation from, reproduction, or publication of this thesis may be granted by my main supervisor, or in his absence, by the Dean of Graduate Studies and Scientific Research when, in the opinion of either, the proposed use of the material is for scholarly purposes.

Any coping or use of the material in this thesis for financial gain shall not be allowed without my written permission.

Student Name: **Abdulsami.A.A.Qawasmi**

Signature:—————————— Date:——————

ACKNOWLEDGEMENT

All Praise is due to Allah, the Lord of the worlds.

Whoever is not thankful to the people, then he is not thankful to Allah. Therefore, I would to take this opportunity to express my sincerest gratitude to all the people who have been supporting me to go forward in my research and studies.

I would like to thank my supervisor, Prof. Sameer Khader, for his ongoing help and supervision during my research. Also, I would like to thank the staff of Faculty of Engineering for their assistance.

Finally, I am glad to thank my friends, family for their help and encouragement.

LIST OF ABBREVIATIONS

PV: Photovoltaic.

MLI: Multi-Level Inverter

CHB: Cascaded H-Bridge

GA: Genetic Algorithm

ANN: Artificial Neural Network

PWM: Pulse Width Modulation

IGBT: Insulated Gate Bipolar Transistor

THD: Total Harmonic Distortion

RE: Renewable Energy

AC: Alternative Current

DC: Direct Current

SDCS: Separated DC Sources

BPA: Back Prorogation Algorithm

MI: Modulation Index

FA: Firefly Algorithm

PSO: Particle Swarm Optimization Algorithm

ABCA: Artificial Bee Colony Algorithm

TLBO: Teaching-Learning-Based Optimization Algorithm

LIST OF FIGURES

LIST OF TABLES

TABLE OF CONTENT

Chapter One
Introduction

1.1. Introduction:

PV power which considered as one of the most RE sources should be converted to AC in order to be connected to electrical network at a desired voltage and frequency.

Inverters are the most important devices used to do that, many different types of inverters are used, each has advantages and disadvantages. Multilevel Inverters (MLI) take place in medium and high power applications, due to lower voltage stress on power semiconductor switches, also it minimizes THD to be more closer to sine wave output, while conventional power inverters can produce two levels output voltages profile.

Multilevel inverter must connected to PV string where shading could change the voltage of given level which in turn cause additional THD generated and voltage Stress across devices

This problem has to be solved by applying programmable PWM for CHBMLI using Artificial Neural network which respond to change in level voltage by adjusting the switching angles of MLI to maintain minimum THD.

1.2. Problem statement

Scientific literature does not contain any reports that deal with wide range of DC source variation caused by shading; most researchers consider 10% of source variation only, therefore, this research

generate switching angles for eleven CHBI Using ANN under wide range of input DC variation up to 40% (18 to 40 volts)

1.3. Objectives:

- We investigate the capability and accuracy of GA to solve nonlinear equations
- We investigate the reliability and accuracy of ANN to generate the CHB 11 level inverter switching angles under different sets of variable DC sources.
- We investigate the output voltage THD at balanced and unbalanced DC sources
- We study the GA and ANN parameters setting effects on output voltage of 11 level inverter

1.4. Thesis structure

A- Build 12x6 solar cells and simulate IV+PV curve.

B- Build 11 level single phase CHBI and drawing the conduction sequence.

C- Using Fourier series to Derive SHE Equations.

D- Write GA algorithm, Set, run, and check THD in CHB.

E- Design suitable ANN topology, train, set parameters and Run.

F- Build PWM Build, calculate conduction and delay time.

G- Build matlab model and simulate.

H- Analyze the results using FFT analysis.

1.5. Chapter Summary

This chapter includes the problem statement which is generating switching angles for eleven CHBI Using ANN under wide range of input DC variation up to 40% (18 to 40 volts), the working steps to achieve this target was listed in thesis structure, 8 steps will be implemented to fulfill this thesis.

Chapter Two
Literature Review

2.1. Previous Studies Related to Multilevel Inverters

1- O. Bouhali, F Bouaziz, N. Rizoug and A. Talha,(2013), reported a way of Solving Harmonic Elimination Equations in Multi-level Inverters by using feed forward Artificial Neural Networks (ANNs) based on Back-propagation Algorithm (BPA), but harmonic 11 was high.

2- Priyal Mandil1 and Dr. Anuprita Mishra, (2014)/ Minimization of THD in CMLI using weight improved particle swarm optimization (WIPSO), THD for three phase eleven-level inverter was 4.759%, the single phase was not included

3- Sarika D Patil and Surbhi Patil (2016) a method for calculating switching angles for firing circuit by using Newton -Raphson method**,** microcontroller IC ATMEGA16 is used to generate pulses but THD is not calculated

4- Mitali Shrivastava and Mrs. Varsha Singh, Dr. Swapnajit Pattnaik (2012) reported a way of training ANN off-line using Back Propagation Algorithm (BPA) for many values of MI, THD for three phase eleven-level inverter at MI=0.8 was 9.79%, Newton Raphson method was used to solve the harmonic elimination equations.

5- V.Joshi Manohar, M.Trinad, K.Venkata Ramana (2016) reported comparative analysis of NR and TBLO Algorithms in Control of Cascaded MLI, THD for three phase seven-level inverter at MI=0.95 was 8.86%, for NR and 6.95% for TBLO

6- S. Chatterji and S. L. Shimi (2013) apply Artificial Intelligent (AI) Based Cascade multi-Level Inverter for Smart Nano Grid, THD for three phase eleven-level inverter was 7.34 %

7- Faete Filho, Leon M. Tolbert, Yue Cao and Burak Ozpineci,used genetic algorithms to determine the optimal switching angles for 11-level MLI to keep the fundamental output voltage constant, the output voltage variation is kept around (1%) but THD couldn't be minimized to be 26.7%

8- Mohammed Al-Hitmi , Salman Ahmad , Atif Iqbal ,, Sanjeevikumar Padmanaban and Imtiaz Ashraf (2018), Used Modified Newton–Raphson and Pattern Generation methods to determine the optimal switching angles for three phase11-level MLI, THD was 7.25%

9-Nitesh Kumar Gupta, Dr.R. Mahanty (2015), used (GA) and (PSO) algorithms to generate the best firing angles for single phase 9-level MLI, THD was 12.98% for GA and 12.25% for PSO, and for three phase 9-level MLI, THD was 9.76% for GA and 8.43% for PSO

10- Sihem. Ghoudelbourk, D. Dib, B. Meghni, and M. Zouli (2017), Modified Newton–Raphson Method to determine the optimal conducting angles for single and three phase11-level MLI, THD was 8.56 % for single phase and 7.46% for three phase

11-Kirti, Manish Kumar Thukral and Vishnu Goyal (2017), implemented an Algebraic method Based Selective Harmonic Elimination of 7-level MLI, then used Artificial neural Networks to fire switching angles, THD was 11.16 % at 0.8 modulation index

12- E. Anandha Banu1 and D. Shalini Punithavathani (2016) used GA to calculate the switching angles then ANN to fire the three phase nine-level Uninterruptible Power supplies (UPS) inverter, THD was 11.83 %

Chapter Three

Multilevel Inverter (MLI)

&

Photovoltaic Cell (PV)

3.1 Introduction

The voltage-source inverters are two levels, i.e. the output voltage either 0 or ± VDC [3].

To get a high quality output Voltage or a current waveform with a minimum amount of THD; they require high switching frequency, many different switching strategies [4] are applied to do so

The problem when using them in high-power and voltage applications is the high modulation frequency, which increases switching losses, also device ratings are determinant. In addition the series and parallel combinations are used to handle high voltages and currents. Due to previous limitations [5] the interest of power industry point to multilevel inverters, in the field of transportation, renewable energy. They are good for use in reactive power compensation; their structures control device voltage stresses which allow producing a high-power and voltage.

To increase the power supplied by MLI you can increase only the number of voltage levels without changing the devices which stand higher voltage or power rating. The special structure of voltage source MLI can produce high voltages with minimum harmonics [6-13].; transformers are not needed as with series devices connected to synchronize switching.

When adding more and more input DC levels, the output voltage waveform harmonic decreases more and more, in single phase CHB inverter which is studied here, we can move from 9-Level to 11-level by adding a block of 4 IGBT's and so on, also the THD will drop**.**

3.2 MLI Topologies

There are three common MLI Topologies [14] as in Fig.(3.1)

1-Diode-Clamped Multilevel Inverter.

2-Flying-Capacitors Multilevel Inverter.

3-Modular Multi-Level Converter (MMC)

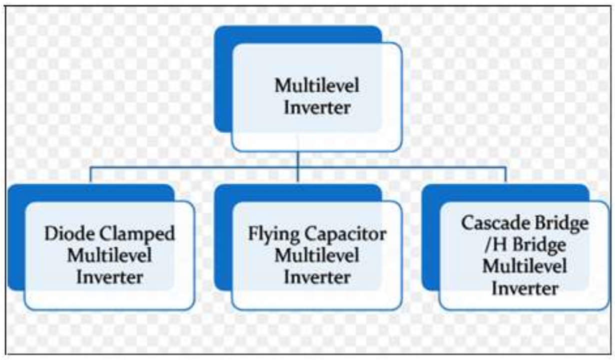

Fig .(3.1) MLI Topologies

3.3. Diode-Clamped Multilevel Inverter

The structure of diode-clamped multilevel (DCMLI) exactly consists of (m-1) capacitors on the DC voltage side and produces m levels on the Ac voltage side.

Fig.(3.2a) shows one leg, and Fig. (3.2b) shows a full bridge five-level DCMLI. The switching devices order is Sa_1, Sa_2, Sa_3, Sa_4, $S'a_1$, $S'a_2$, $S'a_3$, and $S'a_4$.

The four capacitors on DC side marked as, C_1, C_2, C_3, and C_4, the input DC voltage is divided on four capacitors, so each capacitor voltage is fourth of VDC, as with voltage stress through clamping diodes.

The number of devices needed for leg of m-level inverter is:

1- Capacitors (m – 1), 2- Switching devices 2(m – 1), 3- clamping diodes (m – 1) (m – 2).

Principle of Operation

A leg of five DCMLI is shown in Fig.(3.2a), and single phase two legs bridge is shown in Fig.(3.2b).

To explain the construction of output voltage staircase let us consider the DC rail 0 is the reference point.

To produce five-level staircase voltage we do the following:

1. For Vao = VDC, switches Sa_1 through Sa_4 are turned on.
2. For Vao = 3VDC/4, switches Sa_2 through Sa_4 and one lower switch $S'a_1$ are turned on.
3. For Vao = VDC/2, switches Sa_3 through Sa_4, $S'a_1$ and $S'a_2$ are turned on.
4. For Vao = VDC/4, switch Sa_4 and switches $S'a_1$ through $S'a_3$ are turned on.
5. For Vao = 0, switches $S'a_1$ through $S'a_4$ are turned on.

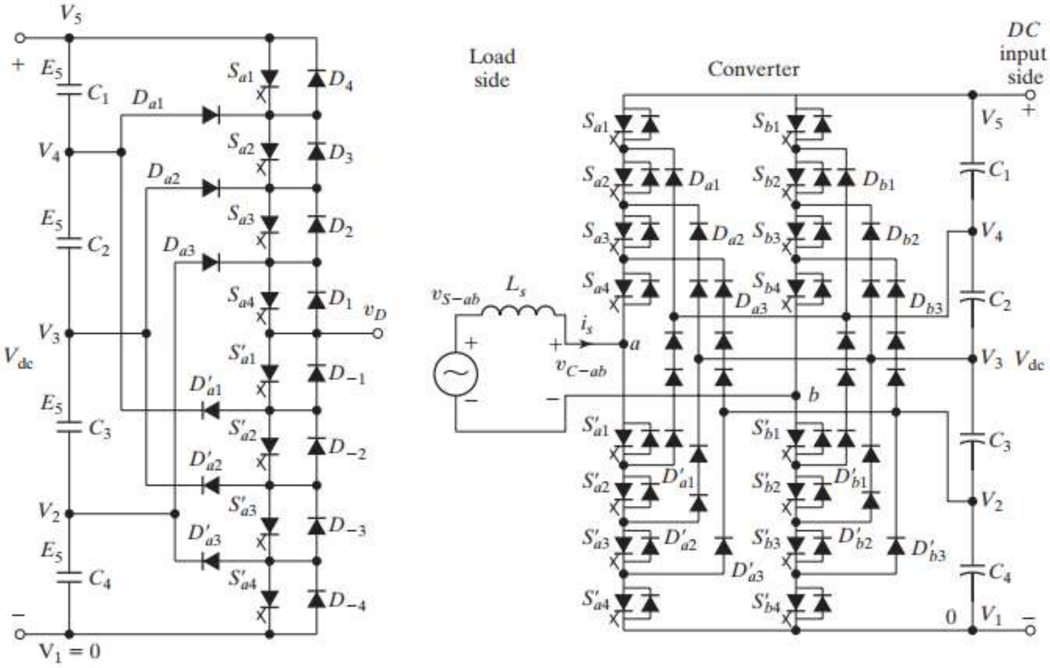

(a) One leg of a bridge (b) Single-phase bridge

Fig (3.2) Diode-clamped five-level bridge multilevel inverter [2].

Table (3.1) shows the output voltage levels and switches operation. It is shown that 4 switches conduct each cycle. The complimentary pairs for one leg are (S_{a1},S'_{a1}), (S_{a2}, S'_{a2}), (S_{a3}, S'_{a3}), and (S_{a4}, S'_{a4}), no one pairs is turned on together in one cycle ,for example if S_{a1} is switched on S'_{a1} will be switched off and so on.

Table (3.1) Voltage levels of Diode-Clamped and their switch status

	Switch Status							
Output Voltage (V_{out})	S_{a1}	S_{a2}	S_{a3}	S_{a4}	S'_{a1}	S'_{a2}	S'_{a3}	S'_{a4}
V_{out} =0	Off	Off	Off	Off	ON	ON	ON	ON
V_{out} =$V_{DC/}$4	Off	Off	Off	ON	ON	ON	ON	Off
V_{out} =$V_{DC/}$2	Off	Off	ON	ON	ON	ON	Off	Off
V_{out} =3/4V_{DC}	Off	ON	ON	ON	ON	Off	Off	Off
V_{out} =V_{DC}	ON	ON	ON	ON	Off	Off	Off	Off

The output phase voltage of five-level inverter is shown in Fig.(3.3). The line voltage consists of nine levels. So output voltage of single phase DCMLI consists of *m*-level and for three phases consists of a $(2m - 1)$ levels.

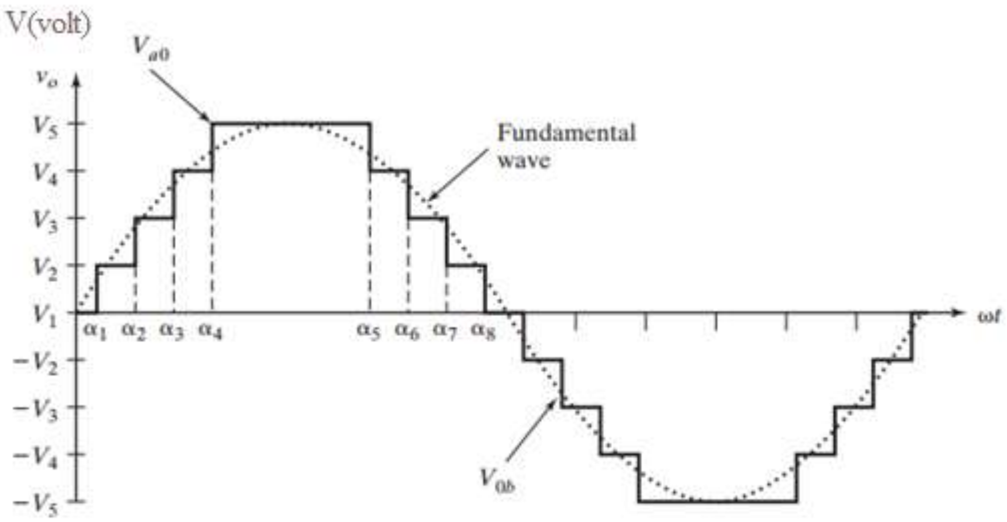

Fig (3.3) Output voltage waveforms of a diode clamped five-level inverter.

3.4. Flying Capacitor Multilevel Inverter (FCMLI).

A single phase, full-bridge, five-level flying capacitors multilevel inverter (FCMLI) is shown in Figure (3.4).

The switching device order is S_{a1}, S_{a2}, S_{a3}, S_{a4}, S'_{a4}, S'_{a3}, S'_{a2}, S'_{a1}.

Capacitors, C_1 through C_4 are connected to DC side and have the same voltage.

Capacitors C_{a1}, C_{a2}, C_{a3} are balancing capacitors for leg *a*, and C_{b1}, C_{b2}, C_{b3} are balancing capacitors for leg *b*.

The ordering number of switches are different from diode clamped inverter, the reason that the sequence of switching conduction are different, which will be explained thoroughly.

There is no difference between diode clamped and flying capacitors inverters, both of them produce the same voltage level, the phase and line voltage have levels are same .

All capacitors and switching devices rate the same voltage; the DC side requires capacitors for an *m*-level inverter equal to $(m - 1)$. For AC side the capacitors needed for one phase is calculated as follows:

$NC = \sum_{j=1}^{m}(\mathbf{m} - \mathbf{j})$, thus, for $m = 5$, $NC = 10$.

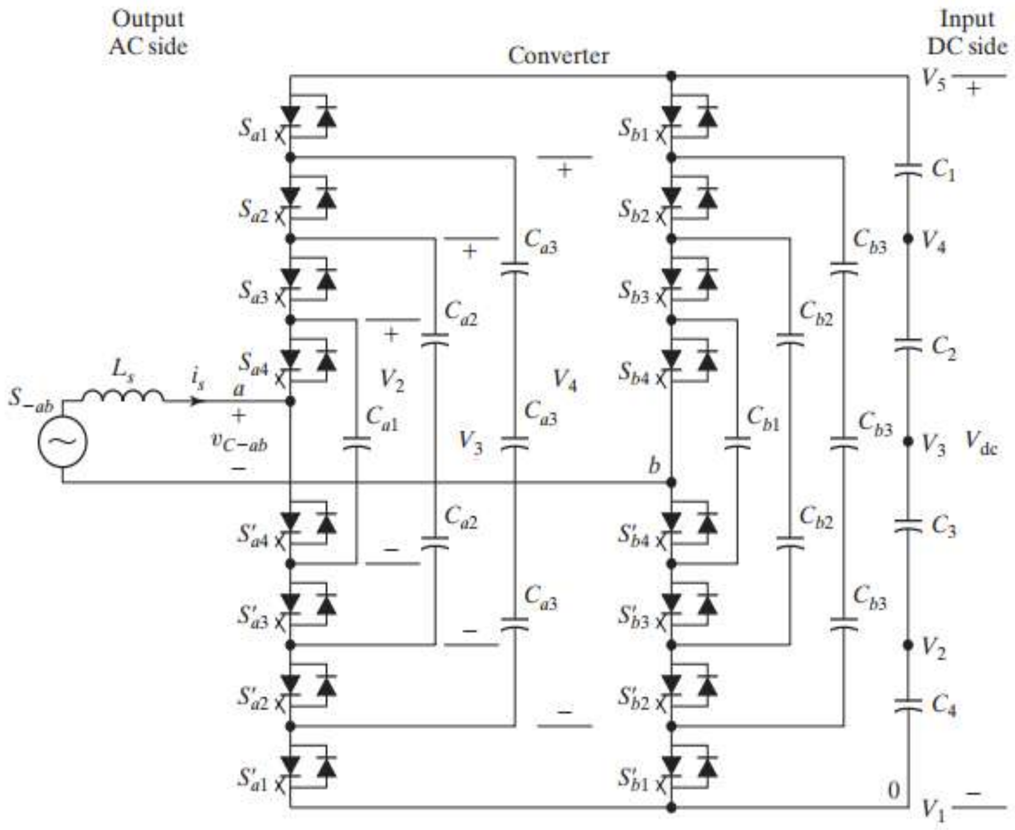

Fig (3.4) A single-phase, five-level FCMLI [2].

Principle of Operation

Referring to Fig.(3.4), the output voltage staircase can be produced considering the DC rail 0 is the reference point as follows.

1-For V*ao* = *V*DC, *Sa*1to *Sa*4 are turned on.

2-For V*ao* = 3*V*DC/4, there are 4 ways:

a. For V*ao* = *V*DC - *V*DC/4, switches *Sa*1, *Sa*2, *Sa*3, *S'a*4 have to conduct.

b. For V*ao* = 3*V*DC/4, switches *Sa*2, *Sa*3, *Sa*4, *S'a*1 have to conduct.

c. For V*ao* = *V*DC - 3*V*DC/4 + *V*DC/2 switches *Sa*1, *Sa*3, *Sa*4, *S'a*2 are turned on.

d. For V*ao* = *V*DC - *V*DC/2 + *V*DC/4 switches *Sa*1, *Sa*2, *Sa*4, *S'a*3 are turned on.

3. For V*ao* = *V*DC/2, there are 6 ways:

a. For V*ao* = *V*DC - *V*DC/2, switches *Sa*1, *Sa*2, *S'a*3, *S'a*4 have to conduct.

b. For V*ao* = *V*DC/2, switches *Sa*3, *Sa*4, *S'a*1, *S'a*2 have to conduct.

c. For V*ao* = *V*DC - 3*V*DC/4 + *V*DC/2 - *V*DC/4, switches *Sa*1, *Sa*3, *S'a*2, *S'a*4 have to conduct.

d. For Vao = VDC - 3VDC/4 + VDC/4, switches $Sa1$, $Sa4$, $S'a2$, $S'a3$ have to conduct.

e. For Vao = 3VDC/4 - VDC/2 + VDC/4, switches $Sa2$, $Sa4$, $S'a1$, and $S'a3$ have to conduct.

f. For Vao = 3VDC/4 - VDC/4, switches $Sa2$, $Sa3$, $S'a1$, $S'a4$ have to conduct.

4. For Vao = VDC/4, there are 4 ways:

a. For Vao = VDC - 3VDC/4, switches $Sa1$, $S'a2$, $S'a3$, $S'a4$ have to conduct.

b. For Vao = VDC/4 switches $Sa4$, $S'a1$, $S'a2$, $S'a3$ have to conduct.

c. For Vao = VDC/2 - VDC/4 switches $Sa3$, $S'a1$, $S'a2$, $S'a4$ have to conduct.

d. For Vao = 3VDC/4 - VDC/2 switches $Sa2$, $S'a1$, $S'a3$, $S'a4$ have to conduct.

5. For Vao = 0, switches $S'a1$to $S'a4$ have to conduct.

Table (3.2): voltage levels of FCMLI and their switch status

	Switch Status							
Output V_{out}	S_{a1}	S_{a2}	S_{a3}	S_{a4}	S'_{a4}	S'_{a3}	S'_{a2}	S'_{a1}
V_{out} =V_{DC}	ON	ON	ON	ON	OFF	OFF	OFF	OFF
V_{out} =3$V_{DC/}$4	ON	ON	ON	OFF	ON	OFF	OFF	OFF
V_{out} =$V_{DC/}$2	ON	ON	OFF	OFF	ON	ON	OFF	OFF
V_{out} =$V_{DC/}$4	ON	OFF	OFF	OFF	ON	ON	ON	OFF
V_{out} =0	OFF	OFF	OFF	OFF	ON	ON	ON	ON

3.5. Modular Multi-Level Converter (MMC)

The MMC topology is shown in Figure (3.5), it consists of six arms, each arm includes N submodules (SMs) connected in series and one inductor

Each SM has two power switches (two IGBTs with anti-parallel diodes) and one capacitor C depending on its gating signals, the SM can provide two different voltage levels.

When S1 is ON and S2 is OFF, the SM provides voltage Vc, the capacitor can therefore be charged or discharged depending on the current direction, if S1 is OFF and S2 is ON, the SM provides 0 volt at the output and the capacitor voltage remains unchanged.

In the blocked state: S1 and S2 are OFF, the capacitor may charge through S1 and cannot discharge.

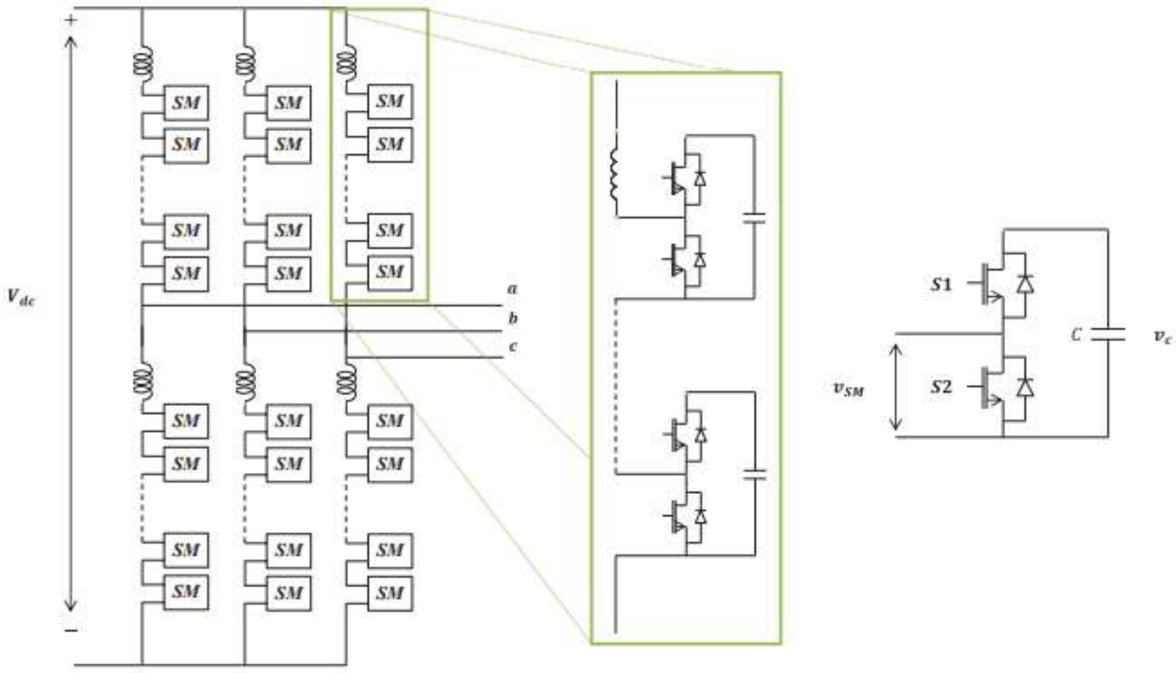

Figure (3.5) MMC Topology [32]

3.5.1 Features of Cascaded voltage H Bridge Multilevel Inverter

The main features can be summarized in the following points:

• Cascaded H bridge inverters need separate DC sources depending on number of its input levels.

• It can be used for different RE sources as hydrogen cells, PV cells, and biomass, because it is supplied from separate DC sources.

The main advantages of the CMLI can be listed as follows:

• It needs the fewest number of devices in comparison with DCMLI or FCMLI to produce the same voltage levels.

• Its structure allow to package each 4 switching devices together as one unit, which facilitate upgrading the number of voltage levels

• Minimum switching losses since it is switched at low frequency.

The main disadvantage of CMLI is it needs separate DC sources, which affect using it.

3.5.2 Cascade Multilevel Inverter Motivation in Solar Applications

A CMLI can be built by connecting series of H-bridges, the number of output levels depend on number of bridges, for *m* input DC sources an (2m+1) output levels produced.

It can be supplied from different separate DC sources (SDCSs), such as PV cells, fuel cells, or batteries; a cascaded H-bridge inverter structure for a single-phase is shown in Figure (3.6a).

This simplified structure without clamping diodes or balancing capacitors make it under interest

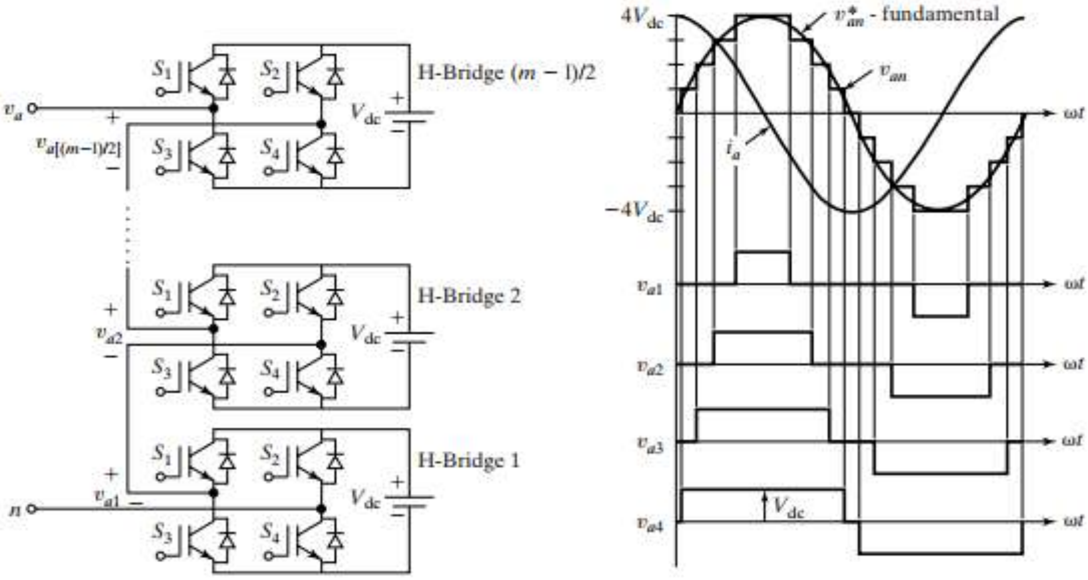

(a) Circuit diagram (b) Output waveform of nine-level phase voltage

Fig (3.6) Single-Phase Cascaded H-Bridge Multilevel Inverter [2].

Principle of Operation

The output voltage waveform of a single phase five level CHBI is shown in Figure (3.6b). Four input DC sources are connected to the bridges, the output voltage is produced by adding input voltages, i.e. $V_{an} = V_{a1} + V_{a2} + V_{a3} + V_{a4}$, any level can be controlled to produce positive, negative or zero voltage, by switching the needed switches from S_1, S_2, S_3, *and* S_4.

If S_1 and S_4 are turned on the voltage produced will be + VDC, if S_2 and S_3 are turned on the voltage produced will be – VDC, finally if all switches conduct the voltage will be 0 VDC

If m considered as the number of input DC sources, the output voltage level for single phase is $N = (2m + 1)$, so, an eleven-level cascaded inverter has to be supplied from 5 input sources,

When CHBI fired with suitable angles the output harmonic distortion can be minimized, in the next chapters we will present the ANN algorithm as technique to minimize THD. The output voltage of CHBI is nearly sinusoidal and the frequency for switching devices is the fundamental frequency.

Figure (3.7b) shows the switching sequence to produce quasi-square wave by firing switches at needed time.

The switching angles or conduction time for each bridge enable it to generate desired voltage level width, by shifting the starting time for each bridge the output voltage will be staircase, each switching device conducts half cycle, which make device stress equal.

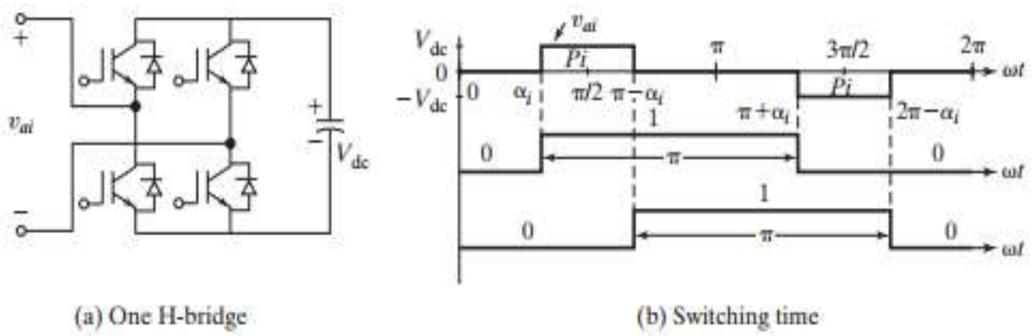

Fig (3.7) Generation of quasi-square waveform [2].

3.6. Comparison of Multilevel Converters

The weight comparison between MLI topologies [15] is shown in Fig.(3.8), it is shown that CHB is the lightest one, then DCMLI, and FCMLI is the heaviest one, also for cost they have the same order as in weight as shown in Fig.(3.9)

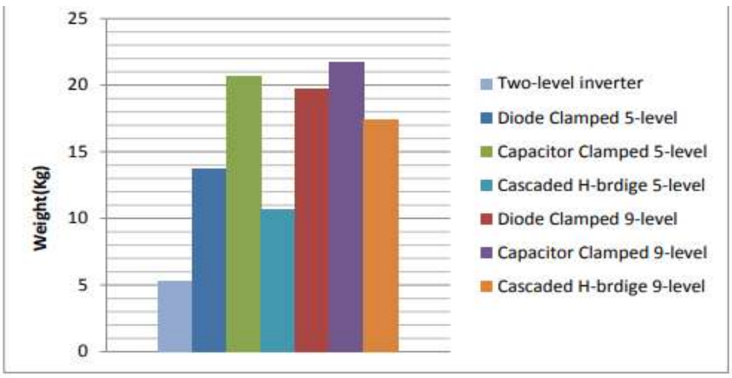

Fig.(3.8) weight comparison between MLI topologies [15]

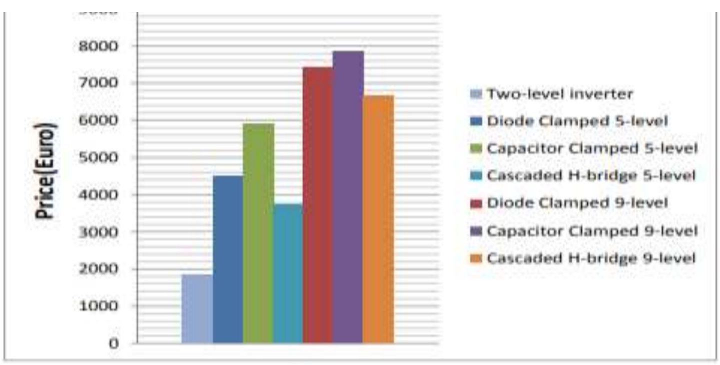

Fig.(3.9) cost comparison between MLI topologies [15]

The number of devices needed for 11 level inverters for 3 topologies are shown in table (3.3)

Table (3.3) Number of devices needed per leg for 11 level inverters

Inverter topology	DCMLI	FCMLI	CHBI
Switching devices	(11 -1) x 2= 20	(11 -1) x 2= 20	(11 -1) x 2= 20
Switch diodes	(11 -1) x 2= 20	(11 -1) x 2= 20	(11 -1) x 2= 20
Clamping diodes	(11 -1) x (11 -2) = 90	0	0
DC bus capacitors	(11-1)=10	(11 -1) = 10	(11-1) / 2= 5
Balancing capacitors	0	(11 -1) x (11 -2)/2 = 45	0

3.7. Eleven-Level Cascaded H Bridge Simulation

Eleven-Level CHB Inverter is built using 20 IGBTs (Fig 3.10a) using Matlab library with specifications as in Fig (3.10b)

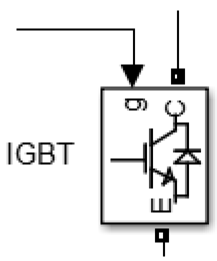

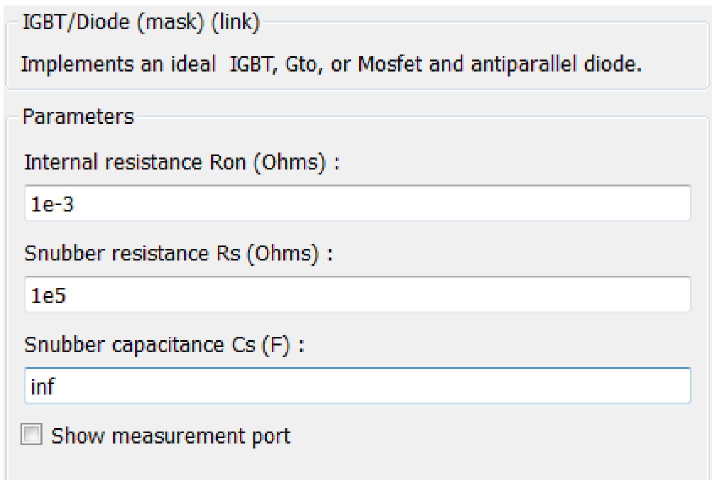

(a) IGBT symbol (b) IGBT specifications

Fig (3.10) IGBT symbol and specifications.

The conduction sequences to produce desired staircase 11 level are illustrated in Fig (3.11) (a-j)

The zero- level which is repeated 3 times requires no switch to conduct.

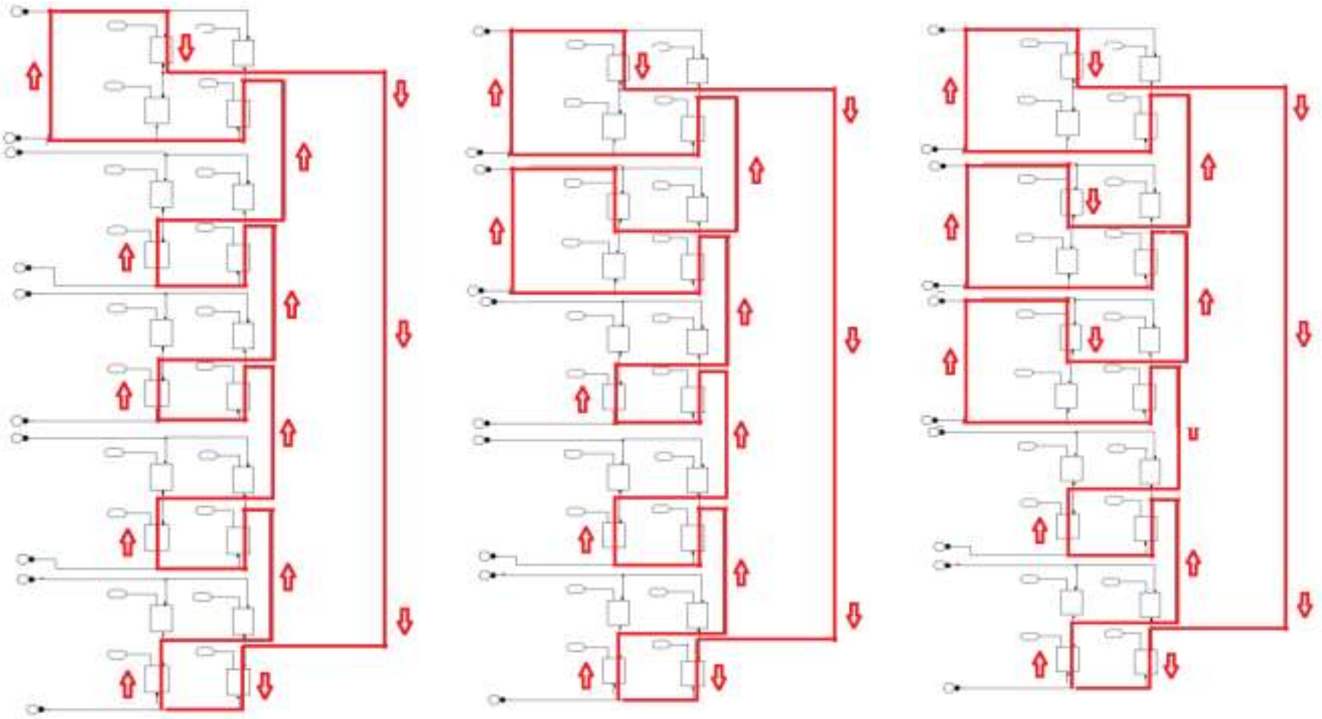

(a) V_{DC1} (b) $V_{DC1}+V_{DC2}$ (c) $V_{DC1}+V_{DC2}+V_{DC3}$

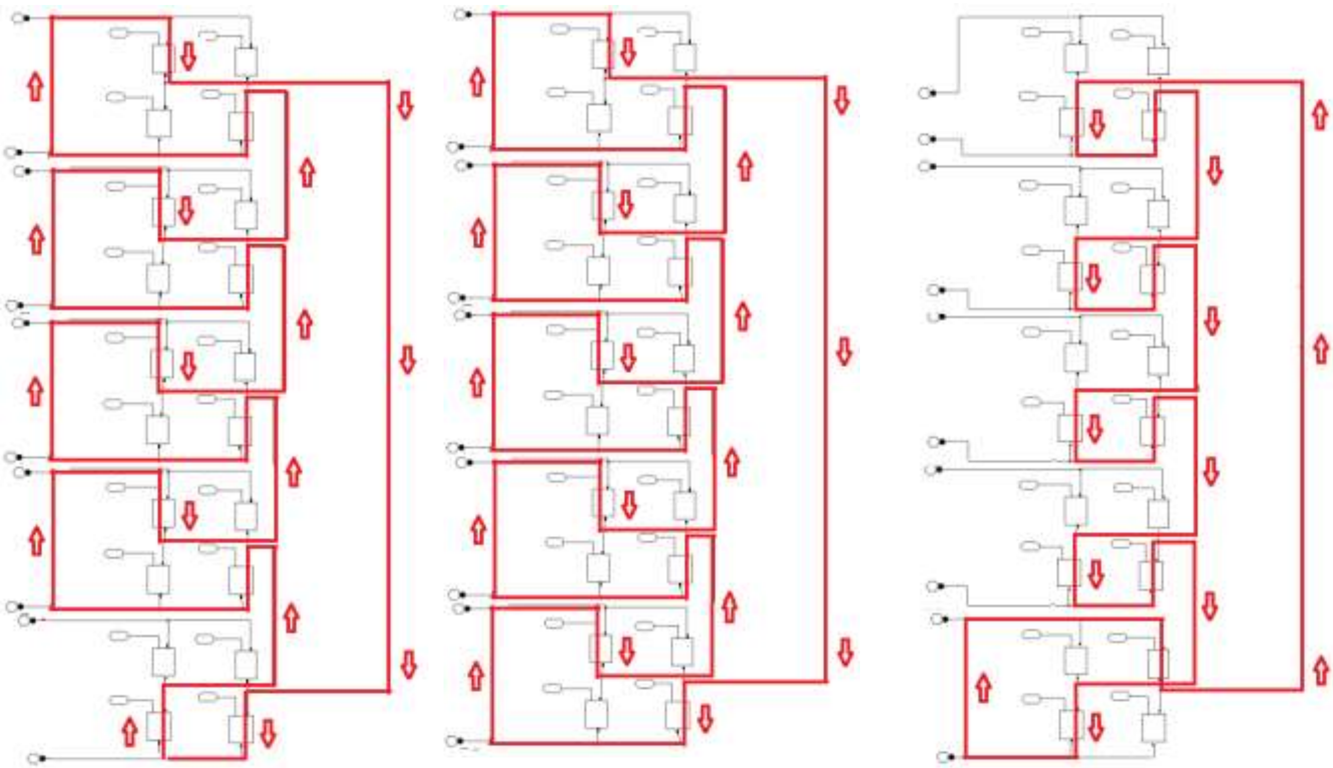

d) $V_{DC1}+V_{DC2}+V_{DC3}+V_{DC4}$ e) $V_{DC1}+V_{DC2}+V_{DC3}+V_{DC4}+V_{DC5}$ f) $-V_{DC1}$

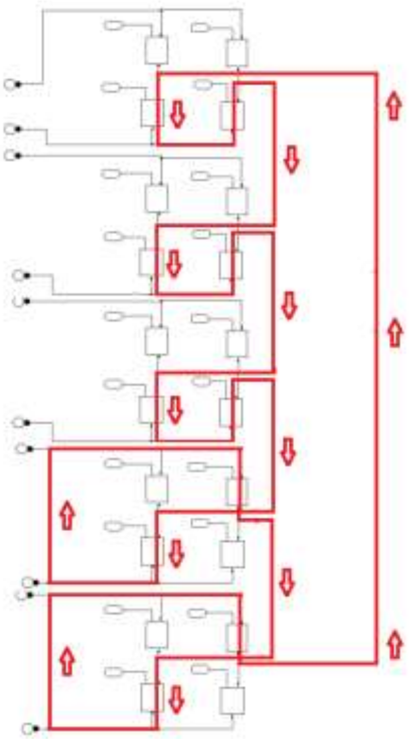

g) – (V_{DC1+} V_{DC2})

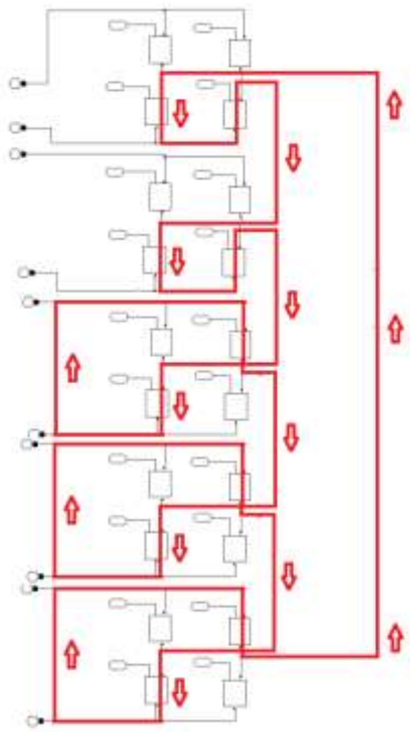

h) – (V_{DC1+} V_{DC2+} V_{DC3})

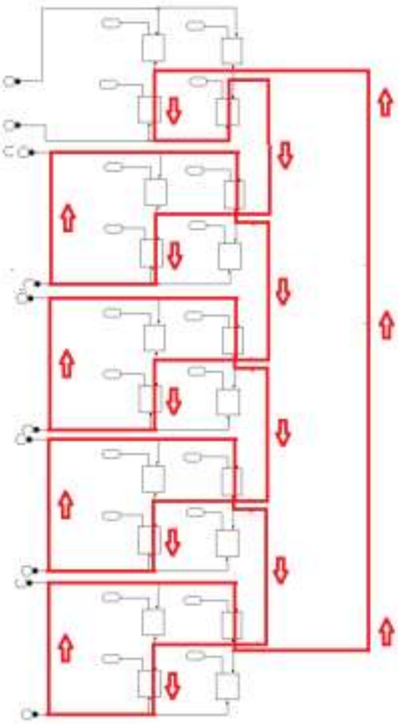

i) – (V_{DC1+} V_{DC2+} V_{DC3+} V_{DC4})

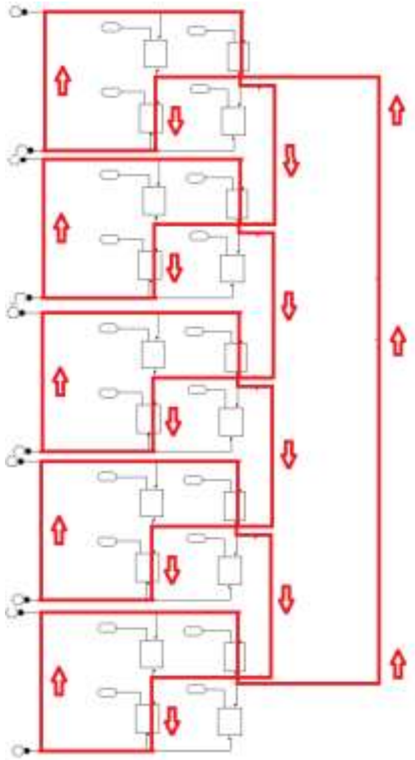

j) – (V_{DC1+} V_{DC2+} V_{DC3+} V_{DC4++} V_{DC5})

Fig (3.11): The conduction sequences to produce 11 level staircase

Matlab Simulation circuit for single phase CHB is shown in Fig.(3.12), (complete circuit is in appendix 7)

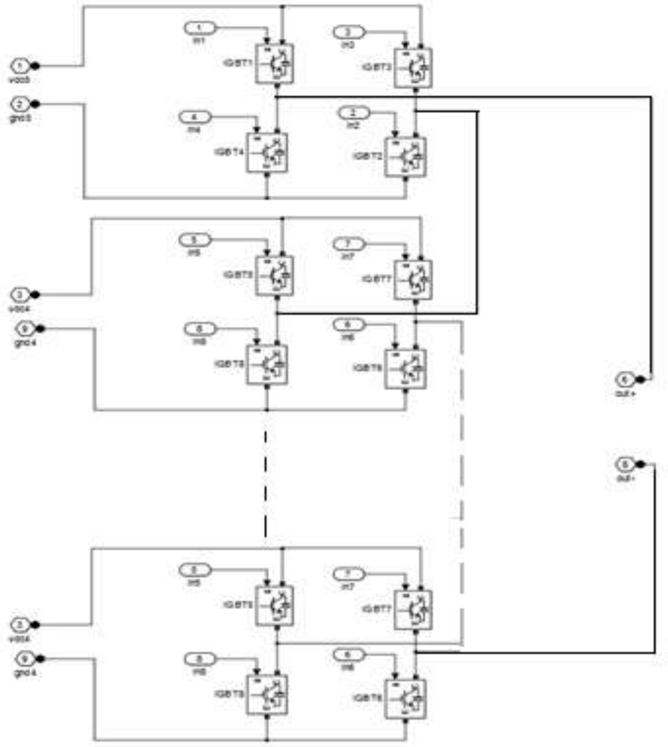

Fig.(3.12) Matlab Simulation circuit for single phase CHB

3.8. PV characteristic and model

3.8.1. Photovoltaic

Converting light energy into electric energy using semiconducting materials is said to be photovoltaic[1].

Sun light photons when hit an electrons in a semiconductor materials deliver them with energy force them to leave their orbits to be free. If a voltage difference is applied, they move in one direction to emerge a current**.**

The first step of manufacturing semiconductors devices was pure crystalline silicon (Si), also Germanium (Ge) is another element is used as a semiconductor material in some devices, both of them have 4 electrons in their orbit, the pure Si and Ge must be doped with boron and phosphorus to perform positive and negative materials.

Semiconductor materials are used to convert sunlight into electricity, nowadays hundreds of electronic and power electronic devices such as diodes, transistors, IGBT's, which are used in renewable energy converters.

Two layers of semiconductor material are made to perform P-N junction, an N-type material is made by doping a silicon atoms with small amounts of Antimony and a P-type material is made by doping a silicon atoms with small amounts of Boron, the two layers then joined together to produce what is generally known as (P-N junction), as shown in Fig. (3.13)

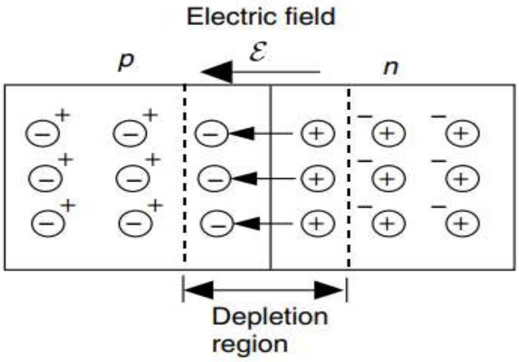

Fig .(3.13) P-N junction

A well known Shockley diode equation (3.1), describes the *(p–n)* junction voltage–current characteristic curve for

$$I_d = I_0(e^{qVd/kT} - 1) \quad (3.1)$$

where: *Id* is the diode current (A),

V_d is the voltage across the diode terminals from the *p*-side to the *n*-side,

I_0 is the reverse saturation current (A),

q is the electron charge ($1.602\ 10^{-19}$C),

k is Boltzmann's constant (1.381×10^{-23} J/K),

T is the junction temperature (K).

When substituting the above constants in Eq. (3.1) gives

$$\frac{qVd}{KT} = \frac{1.602 \times 10^{-19}}{1.381 \times 10^{-23}} \cdot \frac{Vd}{T} = 11600\ \frac{Vd}{T} \quad (3.2)$$

A standard junction temperature of $25C^0$ is used; this minimize (3.2) equation to be

$$I_d = I_0(e^{38.9Vd} - 1) \quad \text{(at 25∘C)} \quad (3.3)$$

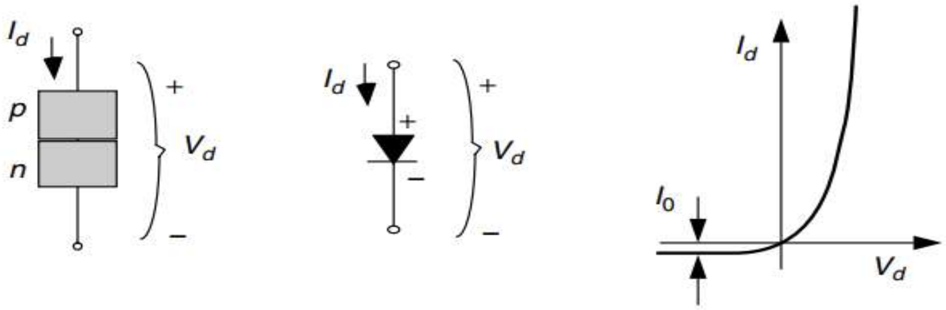

(a) p-n junction diode (b) real diode symbol (c) diode I-V characteristic curve

Fig. (3.14): P-N junction diode

3.8.2. PV Equivalent Circuit:

As shown in Fig.(3.15) the modeling of basic equivalent circuit of the photovoltaic cell can be represented by ideal current source with real diode in parallel with , the solar irradiation is the source of current generation in current source, the lack of irradiation highly affect the current emerged by current source.

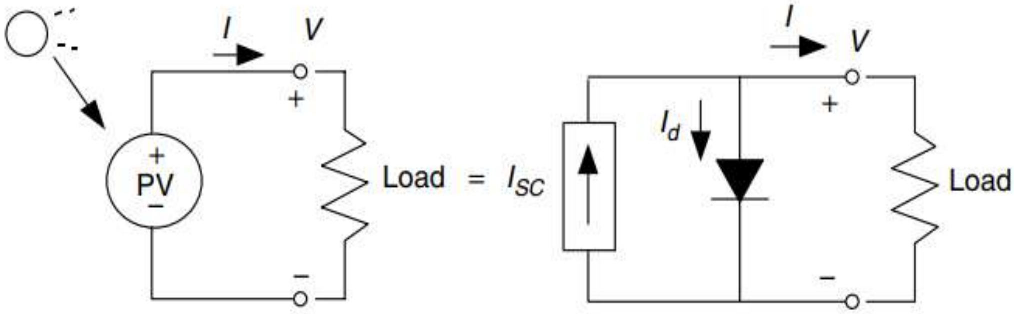

Fig.(3.15): A photovoltaic cell simple equivalent circuit.

Practically two PV parameters must be taken in consideration, first one is known as the short-circuit current, I_{SC}, which represent the current delivered by PV when the load is zero (short circuit), second one is the open circuit voltage, V_{OC} which measure the voltage across the terminals at no load. The two parameters are shown in Fig. (3.16)

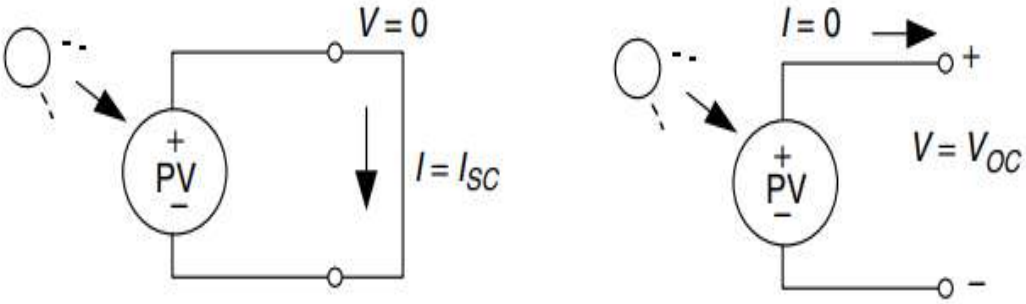

(a) Short-circuit current (I_{SC}) (b) Open-circuit voltage (V_{OC})

Fig.(3.16) PV Short-circuit current (I_{SC}) and Open-circuit voltage (V_{OC}).

The simple equivalent PV circuit is not used in practical; two elements must be added to make it practical, a series (Rs) and parallel (Rp) resistances as shown in Fig. (3.17), so the equation expresses voltage and current is

$$I=I_{SC} - I_0\{exp[\frac{q(V+IRs)}{KT}] - 1\} - \left(\frac{V+IRs}{Rp}\right) \quad (3.4)$$

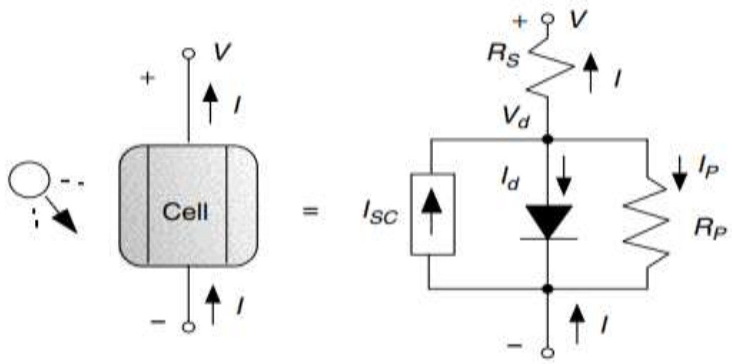

Fig.(3.17) PV cell practical equivalent circuit [Ref. 1]

When the standard condition of a 25◦C cell temperature is considered equation (3.4) becomes

$$I = I_{SC} - I_0[e^{38.9(V+IRs)} - 1] - \frac{1}{Rp}(V+IRs) \quad \text{at } 25°C \qquad (3.5)$$

The I-V characteristic curve plot of Eq. (1.5) *is* shown in Fig. (3.18).

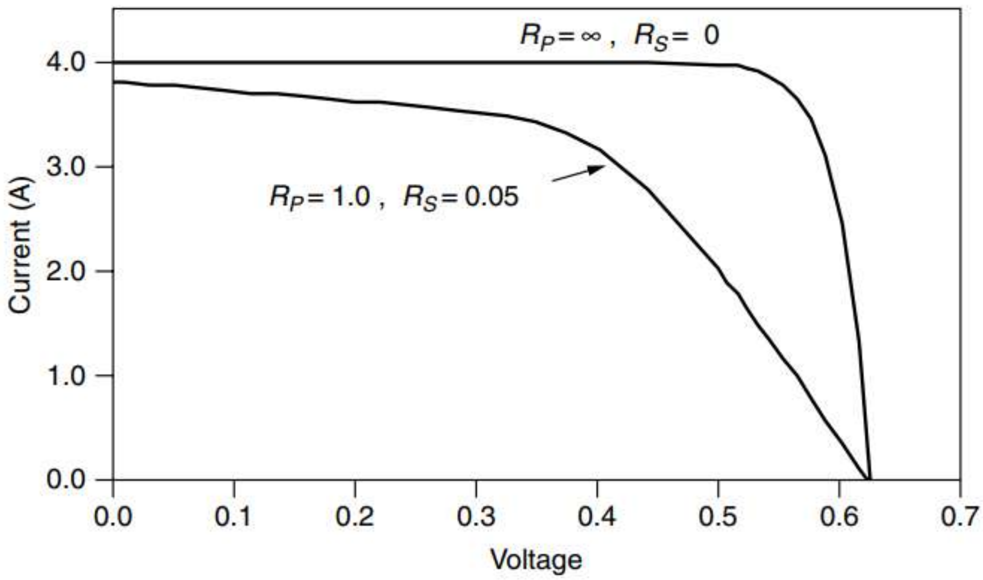

Fig. (3.18) Effects of series and parallel resistances on I-V curve

3.8.3. Shading Impacts on *I-V* Curve

To clarify concealing marvel significance, consider Fig.(3.18) where a n-cell module with current I and yield voltage V gives one cell isolated from the others (appeared as the top cell, however it tends to be any phone in the string). The identical circuit of the top cell has been drawn utilizing its equal circuit while the other (n - 1) cells in the string are appeared as only a module with current I and yield voltage Vn-1

In Fig. (3.19a), the entire of the cells are in the sun and since they are in arrangement, a similar current I pass through every one of them. In Fig.(3.19b), be that as it may, the top cell is concealed and its present source I_{SC} has been decreased to zero.

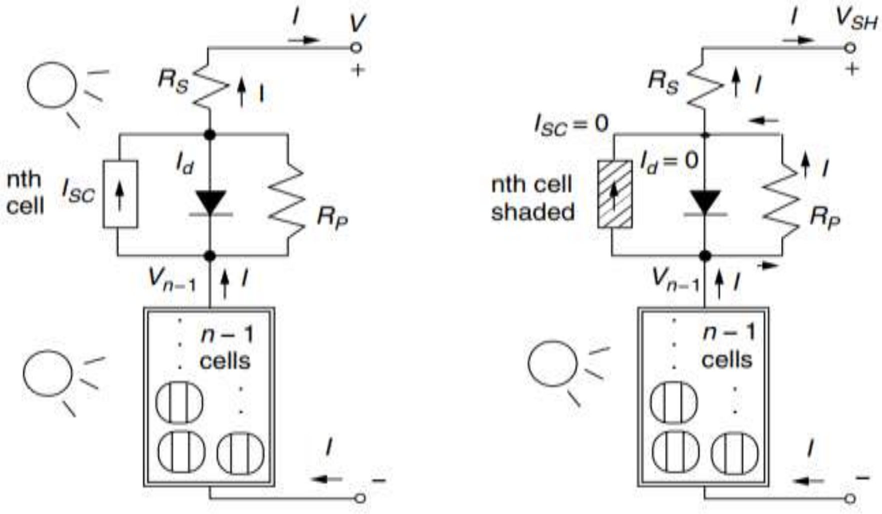

(a) n cells exposed to sun (b) One cell under shading

Fig. (3.19) (a) n cells exposed to sun; (b) one cell under shading [1].

The voltage drop across R_P as current flows through it causes the diode to be reverse biased, so the diode current is also (essentially) zero. That means the entire current flowing through the module must travel through both R_P and R_S in the shaded cell on its way to the load. That means the top cell, instead of adding to the output voltage actually reduces it.

Consider the case when the bottom ($n - 1$) cells still have full sun and still somehow carry their original current I, so they will still produce their original voltage Vn_{-1}.This means that the output voltage of the entire module V_{SH} with one cell shaded will drop to

$$V_{SH} = Vn_{-1} - I\,(R_P + R_S) \tag{3.6}$$

where

$$Vn_{-1} = \left(\frac{n-1}{n}\right) V \tag{3.7}$$

add (1.6) to (1.7) gives

$$V_{SH} = \left(\frac{n-1}{n}\right) V - I\,(R_P + R_S) \tag{3.8}$$

The drop voltage ΔV due to the shaded cell, is given by

$$\Delta V = V - V_{SH} = V - \left(\frac{n-1}{n}\right) V - I\,(R_P + R_S)$$

$$\Delta V = \left(\frac{V}{n}\right) + I\,(R_P + R_S) \quad (3.9)$$

As a result, the module output voltage *(V)* will be (V - ΔV) .

Fig.(3.20) shows the extreme impact on I-V curve, where Rs considered to be zero

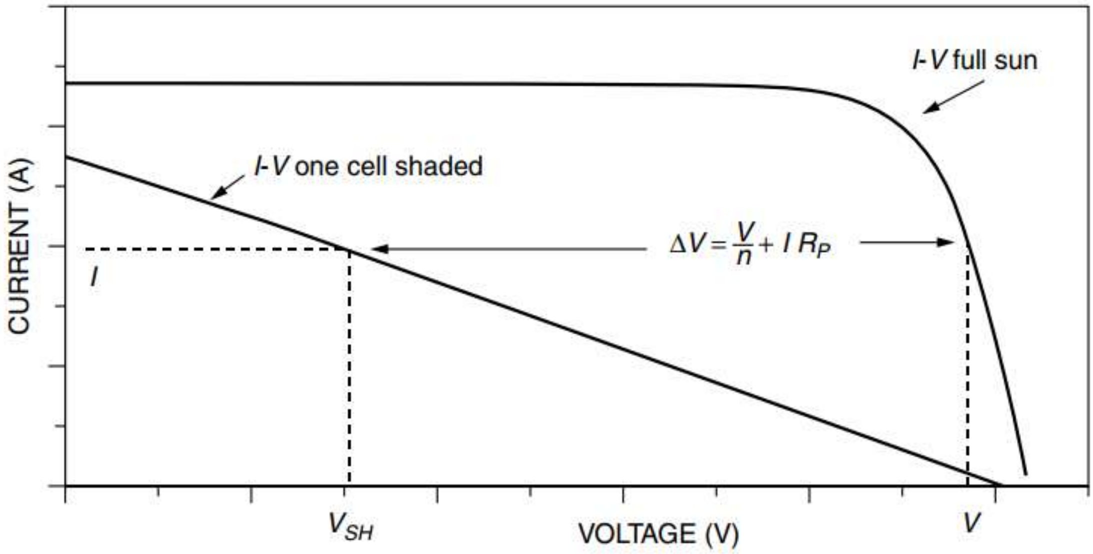

Fig. (3.20) Effect of shading one cell on I-V curve

3.8.4. Bypass Diode for Shade Mitigation

To mitigate the effect of shading external diodes are added to the PV modules. The goal of those bypass diodes is eliminate the voltage drop on shaded cells and find a way for current to flow, which in turn enhance PV output power and voltage .

They are added in parallel with modules to find new way for current, usually three diodes are added since it difficult to add a diode for each cell.

The bypass Diode operates only when solar cell shaded, when the voltage drop increases on shaded cell it conducts permitting the current flows through it, which mean the voltage drop is not more 0.6 volt while if it is not exist high voltage drop occur,

When there is no shading bypass diode will cut off, letting the cell operate normally and the current pass through,

In practical one bypass diode is connected between two series 12 cells terminals, so if one or all of them are shaded the 24 cells will be out of works

Fig (3.21) illustrates the principle of operation for bypass diode

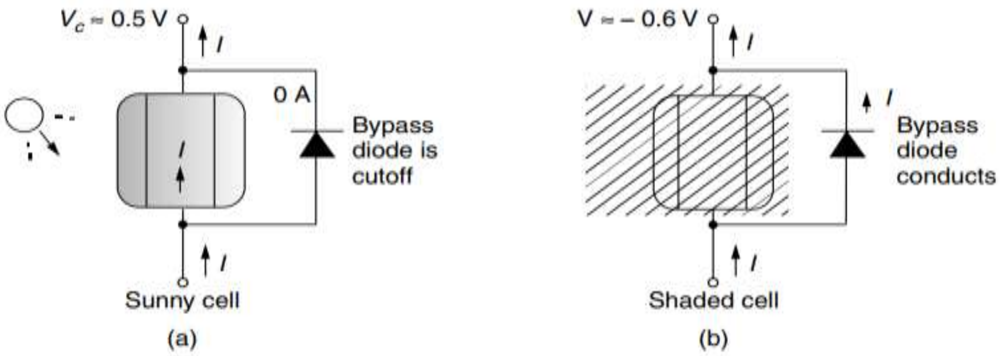

Fig.(3.21) Bypass diode principle of operation.

3.8.5 PV Simulation

The solar cell Fig.(3.22a) is chosen from matlab library with specifications shown in Fig (3.22b)

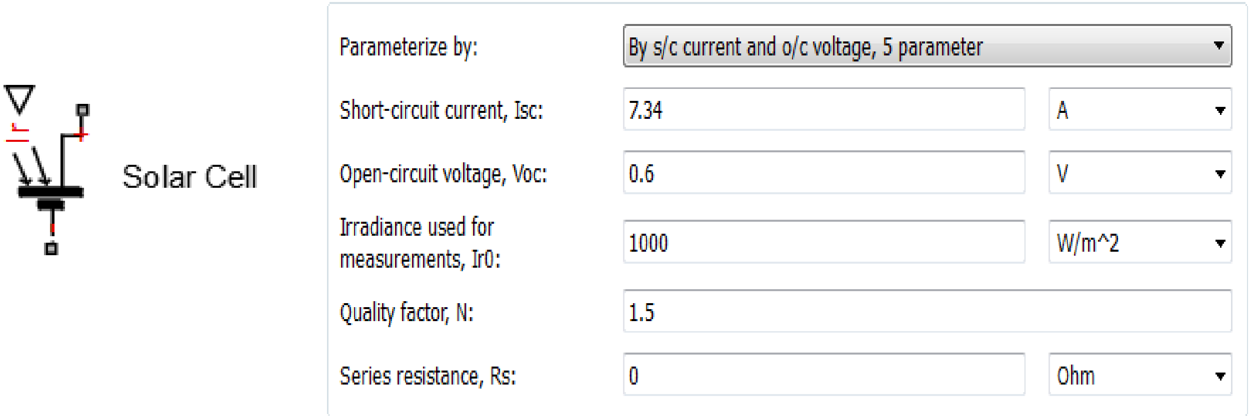

(a) Solar cell Symbol (b) Solar cell specification

Fig. (3.22) Solar cell symbol and specifications.

Each PV panel consists of 6 modules and each module includes 12 solar cells, three bypass diodes added to PV as in Fig (3.23)

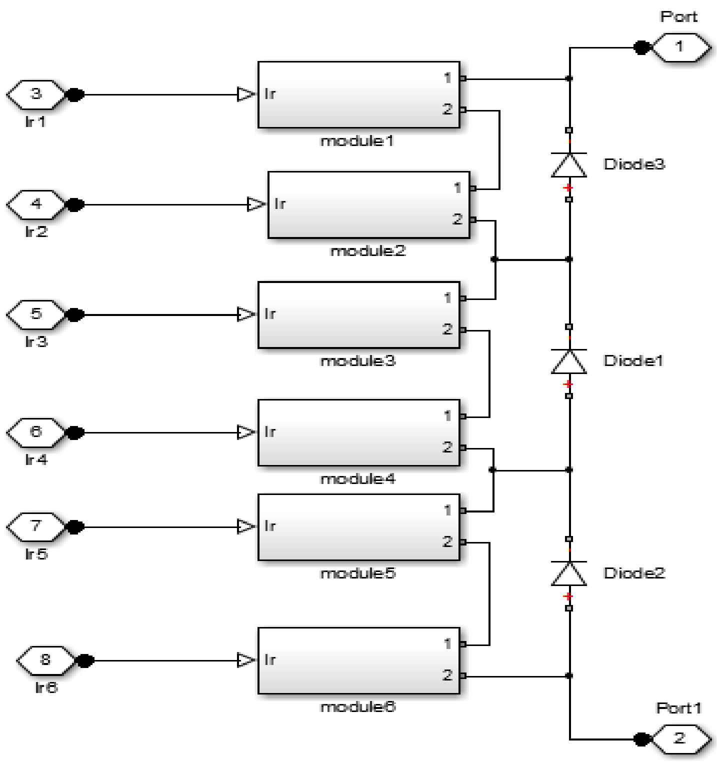

Fig.(3.23) Six PV modules with three bypass diodes

The simulation result for PV module according to Fig.(3.24) under 1000 W/m^2 irradiation produce I-V curve Fig (3.24a) and P-V curve Fig. (3.24b)

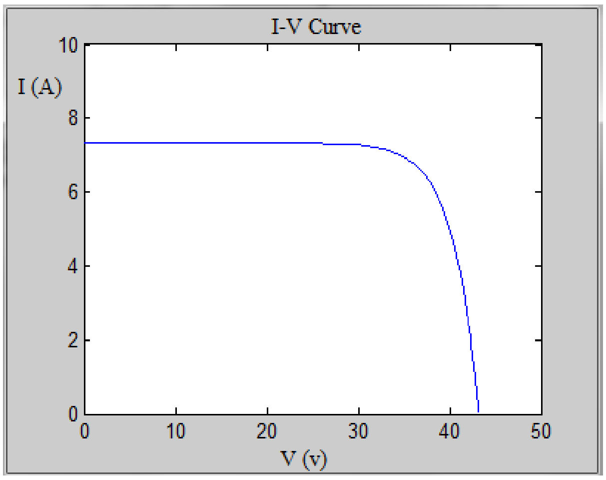

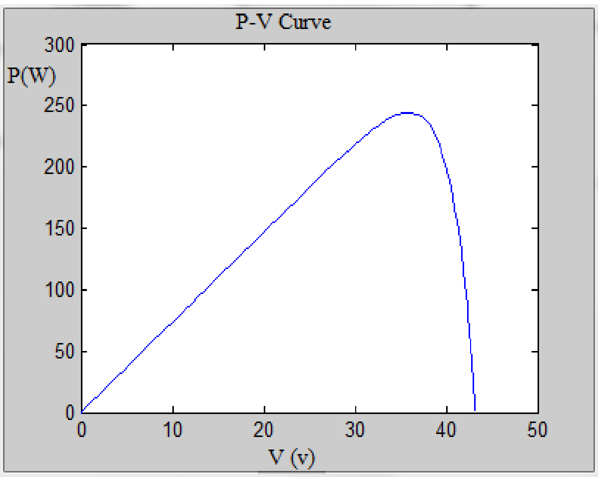

(a) I-V curve (b) PV-curve

Fig. (3.24) I-V curve and PV-curve

The output voltage, current, and power under different values of irradiation are listed in table (3.4), 8 Ω load is chosen to show clearly the voltage drop due to shading

Table (3.4): The output voltage, current, and power under different values of irradiation

Irradiation(W/m^2)	**Voltage (volt)**	**Current(A)**	**Power (W)**
1000	40.02	5.003	200.2
800	37.99	4.749	180.4
600	33.47	4.184	140
400	23.44	2.93	68,68
200	11.74	1.468	17.24

3.9. Chapter Summary

This chapter has provided a brief summary of multilevel inverter circuit topologies and their Switching status, but cannot cover or reference all MLI topologies; the fundamental principle of basic multilevel inverters has been introduced systematically. The intention is simply to provide groundwork to readers.

A comparison of components requirements per leg is done between these three MLI topologies as shown in (Table 3.3)

The concentration was on CHB inverter since it is targeted in this thesis; output voltage levels and switching status are drawn (Fig.3.11 a-j), and Matlab Simulation circuit is implemented as shown in (Fig.3.12)

Chapter Four
Mathematical Analysis & Simulation

4.1. The Fourier Series

A method used to write any periodic mathematical function in the form of a sequence or sum of sine and cosine functions multiplied by a given coefficient [16].

Its name is attributed to the French scientist Joseph Fourier in recognition of his outstanding work in trigonometric series. For any periodic integrable function $f(x)$in the interval [0,2π], $f(\omega t)$ can be written as a sum of sine and cosine functions

$$f(x) = \frac{a_0}{2} + \sum_{n=1}^{N}(a_n \cos(\text{n}\omega\text{t}) + b_n \sin(\text{n}\omega\text{t})) \qquad (4.1)$$

Where Fourier coefficients are given by:

$$a_0 = \frac{1}{\text{T}} \int_0^T f(t)dt$$

$$a_\text{n} = \frac{2}{\text{T}} \int_0^T f(t)\cos(n\omega t)\, dt$$

$$b_\text{n} = \frac{2}{\text{T}} \int_0^T f(t)\sin(n\omega t)\, dt \qquad (4.2)$$

It is shown from Eq.(4.1) that a periodic function can be decomposed into an infinite number of trigonometric components each is multiple of w (nw). These components are fundamental frequency (n=1), a DC component (a_0), and harmonic components (n≥2). For the output square wave of MLI shown in Figure (4.1a), under equal DC sources, the output voltage for first level shown in fig. (4.1) can be written as follows

$a_0 =$ 0, because of wave form symmetry

$a_\text{n} =$ 0, because of odd symmetry

$$b_1 = \frac{2}{\pi} \int_{\theta 1}^{\pi-\theta 1} Vdc\sin(n\omega t)\, d\omega t$$

$b_1 =$

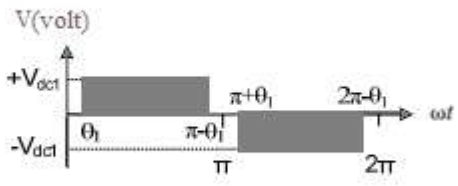

$$\frac{2}{\pi} \int_{\theta 1}^{\pi-\theta 1} Vdc\sin(n\omega t)\, d\omega t$$

Fig.(4.1) first level of output voltage

$$b_1 = \frac{-2Vdc}{\pi}\,[cosn(\pi - \theta 1) - cosn(\theta_1)]$$

$$b_1 = \frac{-2Vdc}{\pi}\,[-2cosn(\theta_1)]$$

$$b_1 = \frac{4\,Vdc}{\pi}\,[cosn(\theta_1)\,] \qquad (4.3)$$

Substituting (4.3) in (4.1) gives

$$V(\omega t) = \frac{4\,Vdc}{\pi}\sum_{n=1,3,5}^{N}\frac{cosn(\theta 1)\,\sin(n\omega t)}{n} \qquad (4.4)$$

For an eleven-level CHB which needs five switching angles, the output voltage with balanced input sources as shown in figure (4.2a) become:

$$V(\omega t) = \sum_{n=1,3,5}^{N}[\frac{4\,Vdc}{n\pi}((cosn(\theta 1) + cosn(\theta 2) + \cdots + cosn(\theta 4) + cosn(\theta 5))]\sin(n\omega t)) \qquad (4.5)$$

For unbalanced input DC sources as shown in figure (4.2b) the output voltage will be:

$$V(\omega t) = \sum_{n=1,3,5}^{N}[\frac{4}{n\pi}((\mathrm{VDC1}\,cosn(\theta 1) + \mathrm{VDC2}\,cosn(\theta 2) + \cdots + \mathrm{VDC5}\,cosn(\theta 5))]\sin(n\omega t)) \quad (4.6)$$

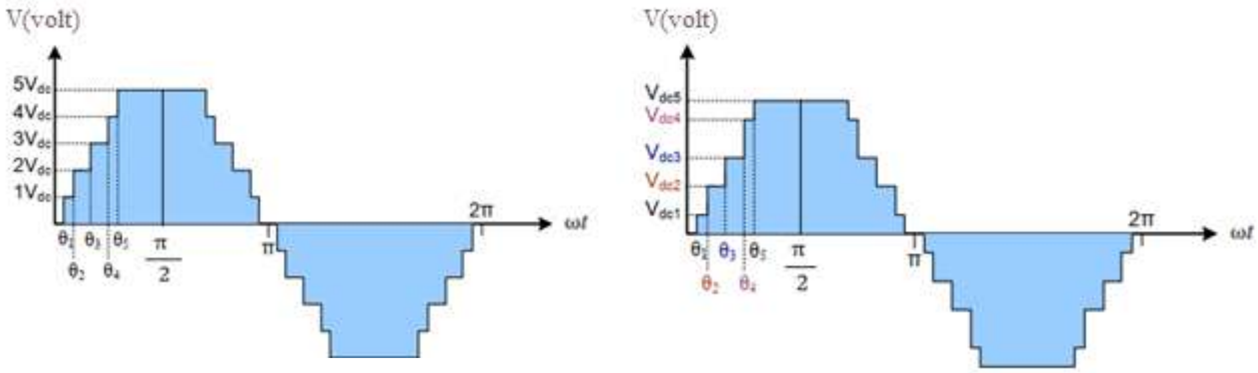

(a) Output waveform for balanced DC source (b) Output waveform for un balanced DC source

Figure (4.2) Output waveform for 11 level CHBI

4.2 Selective Harmonic Elimination for balanced and Unbalanced DC Sources

Referring to Eq.(4.6), the output voltage can be written to have the fundamental voltage when (n=1) and harmonic components when (n>1). Each harmonic of the output voltage can be expressed by:

$$V_{nth}(\omega t) = \sum_{n=1,3,5}^{\infty}[\frac{4}{n\pi}((V_{DC1}\,cosn(\theta_1) + V_{DC2}\,cosn(\theta_2) + \cdots + V_{DC5}\,cosn(\theta_5))\sin(n\omega t))] \qquad (4.7)$$

where V_{DC1} is the voltage level of first DC source, θ_1 is the switching angle of first DC source (V_{DC1}), θ_2 is the switching angle for second DC source (V_{DC2}), and so on. The five angles θ_1 to θ_5 in Eq. (4.7) will be used to formulate the five equations needed to find the fundamental voltage and minimize the first four harmonics [17], in unbalance DC sources modulation index is not targeted since the set of switching angles vary corresponding to DC sources variation, so the fundamental harmonic will be set to 110 V or 120 V as in Eq.(4.8).

$$V_{fun\,(rms)}\,(\omega t) = \frac{4}{\pi\sqrt{2}}\left(\left(V_{DC1}\cos(\theta_1) + V_{DC2}\cos(\theta_2) + \cdots + V_{DC5}\cos(\theta_5)\right)\right) = 120\ \text{V} \qquad (4.8)$$

In three phase inverter 3rd and 9th harmonics are cancelled directly, but in single phase they must be included, since we focus on eleven level inverter, five equations can be solved, they are the first four harmonics 3rd, 5th, 7th, and 9th in addition to fundamental equation.

The set of equations are Eq.(4.8) for fundamental and Eq.(4.9) for harmonics

$$V_{k\,(rms)}\,(\omega t) = \frac{4}{k\pi\sqrt{2}}\left(\left(VDC1\cos(k\theta 1) + VDC2\cos(k\theta 2) + \cdots + VDC5\cos(k\theta 5)\right)\right) = 0\ \text{V} \qquad (4.9)$$

Where K = {3,5,7,9}

The above equations are nonlinear; therefore, when they are solved many sets of solutions will appear.

In GA, the problem with local minima will increase numbers of trials to get the best solution, but GA will generate approximate solution if the exact solution are not exist while numerical methods can't do that.

4.3. Genetic Algorithm (GA)

Genetic algorithm is a method of optimization and research. This method can be categorized as an evolutionary algorithm [18] that relies on the imitation of nature's work from a Darwinian perspective.

The GA uses a search technique to find controlled or approximate solutions that optimize. It is classified as global search heuristics. It is also a specific class of evolutionary algorithms, also known as evolutionary computation, which uses technology inspired by evolutionary biology [19] such as inheritance, mutations, selection and crossover.

In our problem, different analytical algorithms were used, as Newton–Raphson, but those methods can't return an answer if there is no exact solution for the equations.

Genetic Algorithm is used to deal with complex problems when analytical methods are impractical [20-21].

The code written in GA allows it to find the closest solution (set of angles) if the exact solution is not existing, GA operator will minimize the total harmonic distortion THD not cancelling it, this mean no probabilities to receive no solution, but many trials must done to get best fitness value which is closest to zero, fitness value zero means the exact solution is achieved.

The GA program is written in m-file using Matlab R2013a, it's divided into three parts, fitness file, constraints file, and main file

a) Fitness file includes the total harmonic distortion (THD) which to be minimized

$$\mathrm{THD} = \frac{1}{\mathrm{V1}}\left(\sum_{n=3,5,\ldots}^{\mathrm{N}} \mathrm{V}n^2\right)^{1/2} \quad (4.13)$$

where V_1 is the fundamental harmonic voltage,V_3;V_5; . . . ; V_n are the 3 rd 5th; 7th; . . . ; nth order is harmonic voltages. The Matlab file is shown in appendix (1)

b) Constraints file includes the constraints conditions, first the 3 rd 5th; 7th; 9th harmonic equations equal zero and second the switching angles satisfy the condition

$$0 < \theta 1 < \theta 2 < \theta 3 < \theta 4 < \theta 5 < \frac{\pi}{2}$$

The Matlab file is shown in appendix (2)

c) Main function includes GA operator and parameters like crossover, mutation, population size and generation, The Matlab file is shown in appendix (3)

GA flowchart that solve the problem is given in Fig (4.3)

Many trials of setting parameters and running program had been done so the program

doesn't stop or fall in local minima, and return best result, it found the population size and generation must be changed each set of input voltage DC as (800, 70) or (750, 30) respectively, since not any values can give the best results.

When the program stops , a fitness value of $3.28 * 10^{-6}$ is returned, when its value equal zero this mean an exact value of solution reached, but here an approximate value were got and the program stops and generate the best set of angles, here, the number of generation is set to be the stopping parameter.

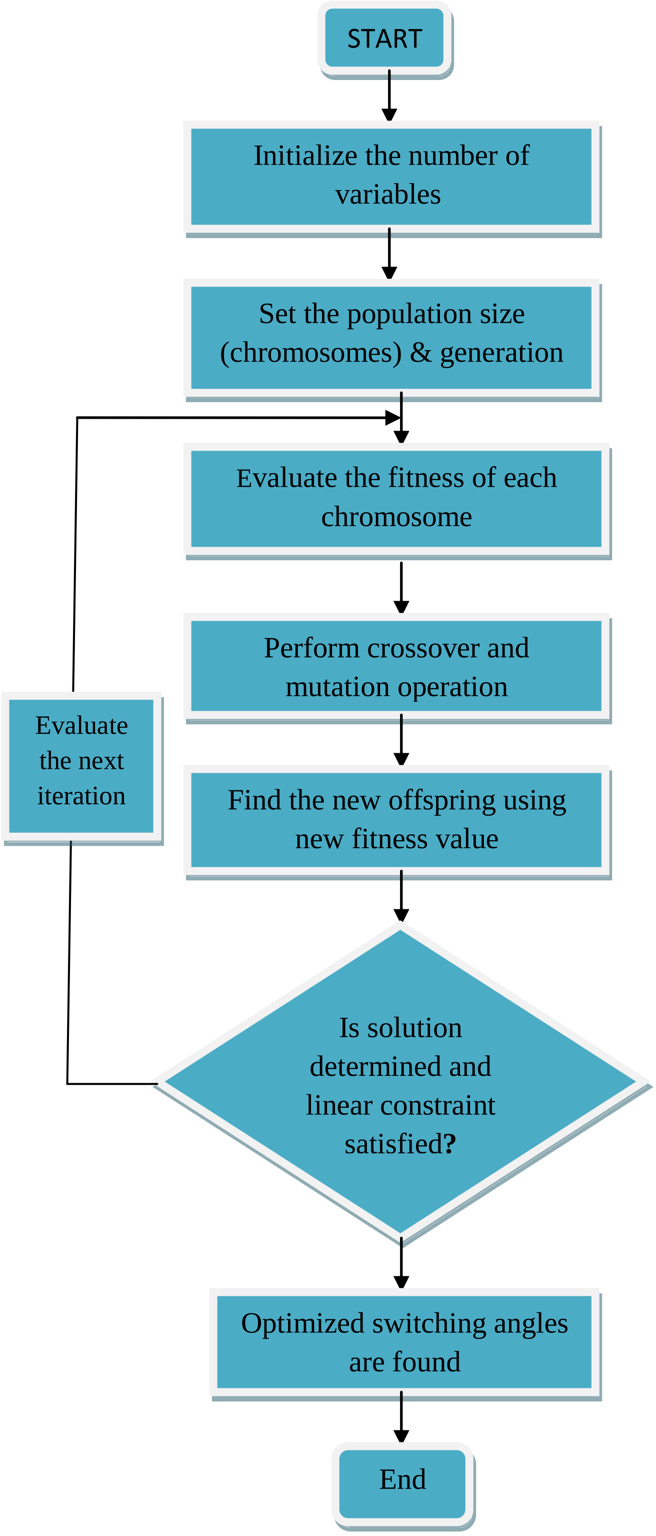

Fig (4.3) GA flow chart

After 20 generations, an approximate solution is done, but since no stopping parameter, the program continue to next generations to enhance the results, until finishing after 70 generation, Fig.(4.4) shows the algorithm best and mean fitness .

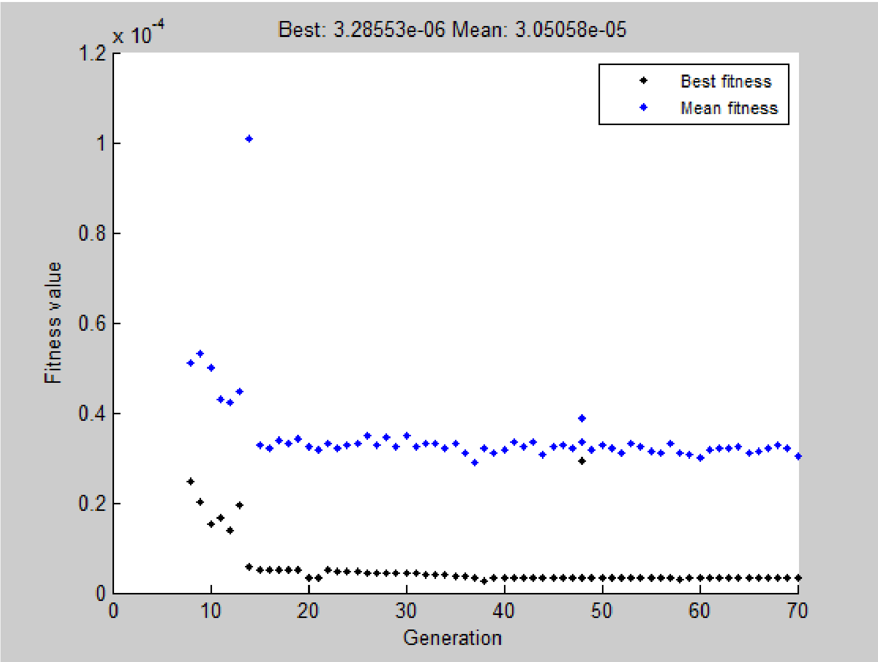

Fig .(4.4) GA average and best fitness

The output results for sample sets of voltages and their angles are shown in table (4.1), those voltages and angles sets will be used to train the ANN

Table (4.1): GA outputs results

	V_{DC} (volt)	Θ(degree)	**Fitness Value**			V_{DC} (volt)	Θ(degree)	**Fitness Value**
unequal VDC	39	8.560	0.0187		unequal VDC	31	9.093	0.0277
	38	21.601				33	19.384	
	37	38.131				35	36.246	
	36	59.154				37	58.392	
	35	88.742				39	89.000	
unequal VDC	18.35	8.772	0.052		equal VDC	39	8.738	0.231
	22.22	14.084				39	20.753	
	27.19	18.221				39	37.421	
	40.03	36.940				39	58.73	
	38.56	60.202				39	88.788	

4.4. Artificial Neural Network (ANN)

ANN is computational techniques which simulate the human brain [22] way dealing with tasks through a massive parallel processing, made up of simple processing units, it stores practical knowledge and empirical information to enable user adjusting the weights.

ANN is used in engineering many applications, like pattern recognition, control, classification, and other applications [23-26], It is used here due to its capability to fit nonlinear complicated problems that need intensive calculation [27]. Artificial neural network architecture is how to connect neurons to each other, which is related to the training algorithm.

Each neuron has a collector joint that combines the weighted input with the displacement to form the numerical output of the neuron, as a result, the neuron layer output compounds form the output beam (a single-column array), and the relationship that gives this output.

So instead of using a lookup table to store the large amount of informations, ANN will be alternative.

The problem you will face is to know how many hidden layers needed and how many neurons in each layer to train ANN which depend on your problem, there is no one topology for all problems. The complexity of relation between input and output, and number of inputs and outputs are the main factors, you can't determine those factors directly, and you have to try many times to achieve the desired topology.

GA can used to solve a specific number of set of input voltage, and it is impossible to find all suitable angles for all DC variation, thus ANN is used to generate a suitable set of firing angles depending on any variation in DC input voltage.

The training process consume too much time, tens of trials may be done to get best result, but when apply it in matlab it will generate the angles quickly.

After tens of trials, the final topology was a feed forward ANN, consists of two hidden layers. The final topology is shown in Fig.(4.5)

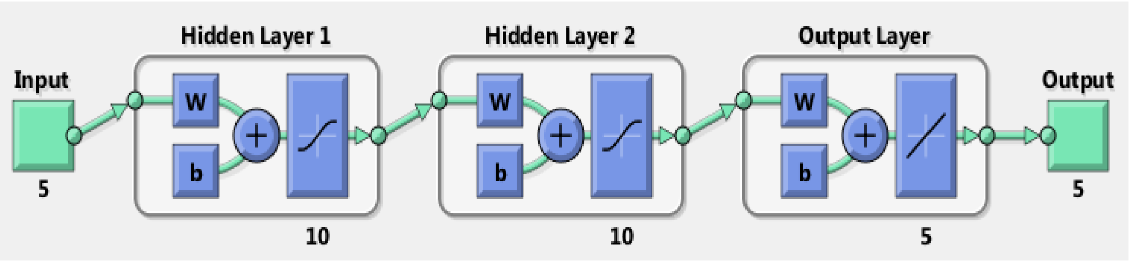

Fig.(4.5) ANN topology

The network training program is written in m-file using Matlab R2013a, many parameters were set to get best training. The two hidden layers have 10 neurons with TANSIG activation function for both, while PURELIN activation function is used for output layer as shown in Fig (4.6), mean squared error (MSE) can give help you to judge if you are right or not.

$$MSE = \frac{1}{p} = \sum_{i=1}^{p} \left| y^i - d^i \right|^2 \qquad (4.16)$$

Where,

p: data entries number

y: ANN output vector

d: needed output vector

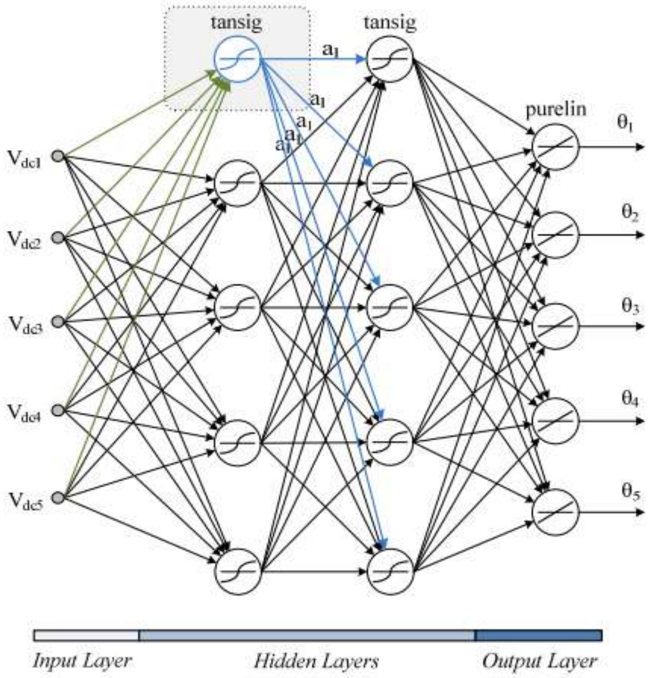

Fig (4.6) Multilayer feed forward ANN topology

The training parameters and Algorithms are changed repeatedly to achieve the best training performance, and many training trials were done to get the best one, traingda (Gradient Descent with Adaptive Learning Rat) gives the best regression we need, while the other training algorithms don't satisfy the best regression.

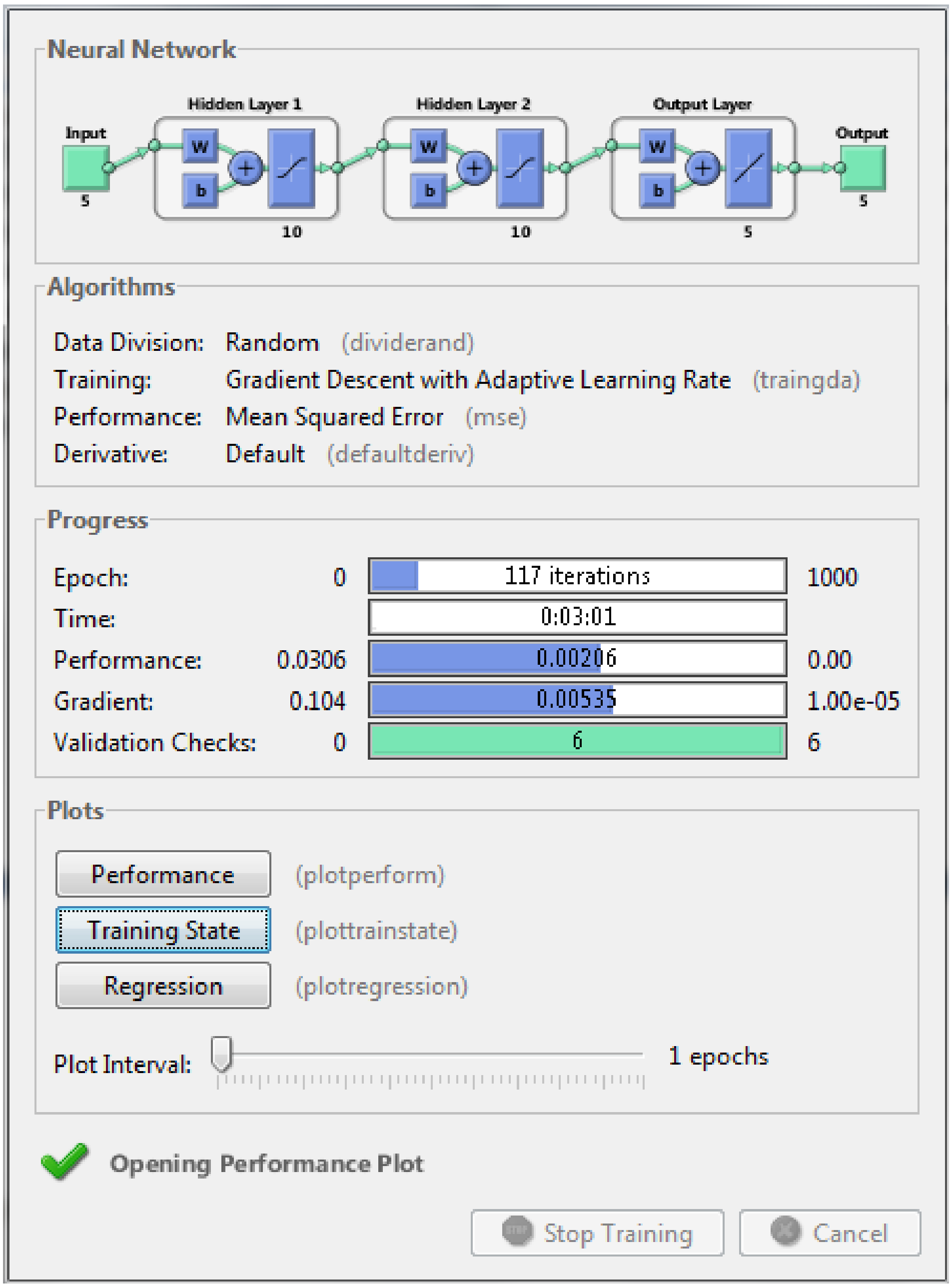

Fig (4.7) ANN Training

The ANN code including parameters is shown in appendix (4)

The training process is shown in Fig (4.7), it stopped after 117 iterations when validation checks is achieved, the training performance is shown in Fig (4.8), the final regression was 99% as shown in Fig (4.9)

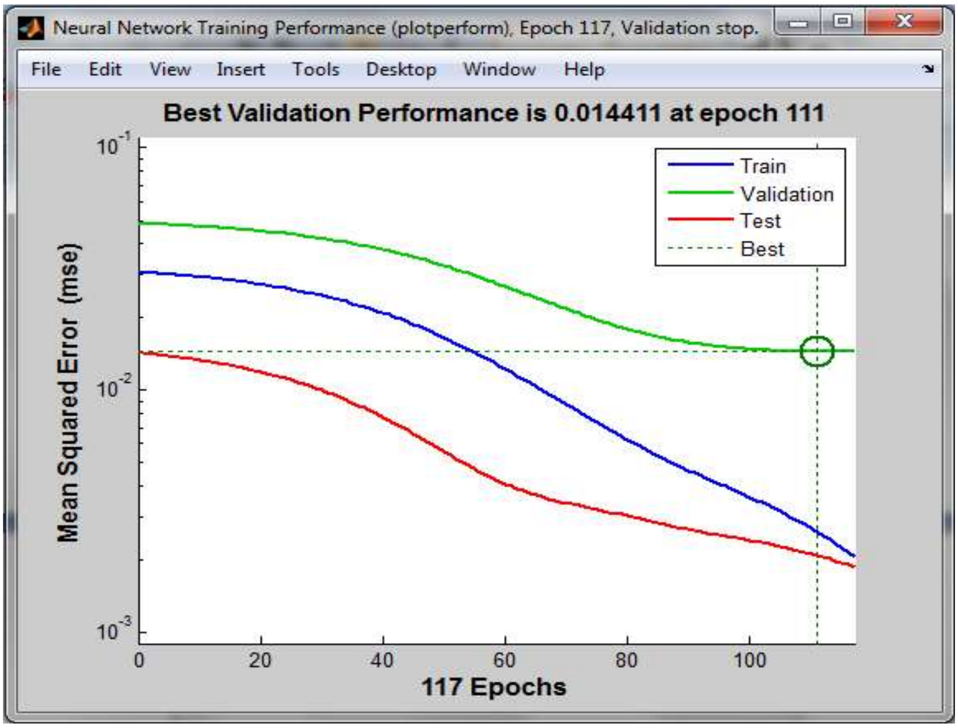

Fig (4.8) ANN Training performance

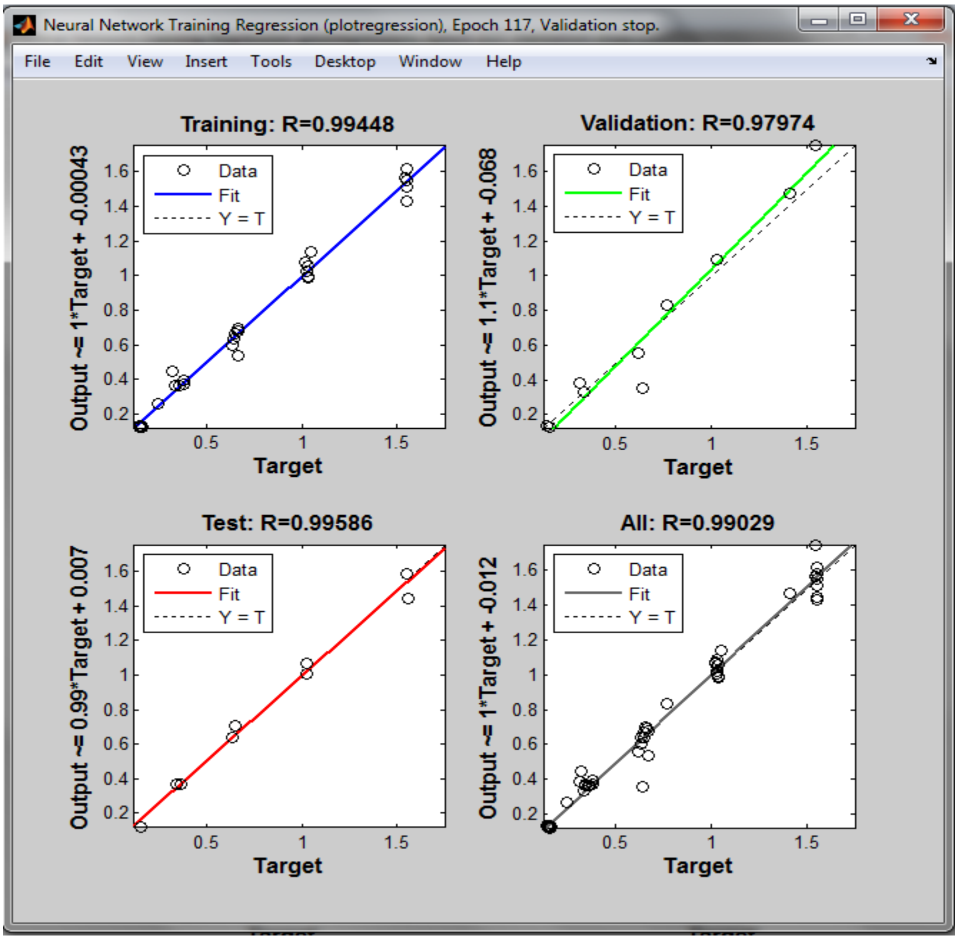

Fig (4.9) ANN Training regression

4.5. Pulse Width Modulation

The ANN are trained to produce five firing angles in radian depending on the DC sources levels as shown in Fig (4.10) [8], the number of IGBT's needed for eleven level inverter are 20 IGBT's (2n+1) pulse width modulator will generate the conduction, delay time for each IGBT

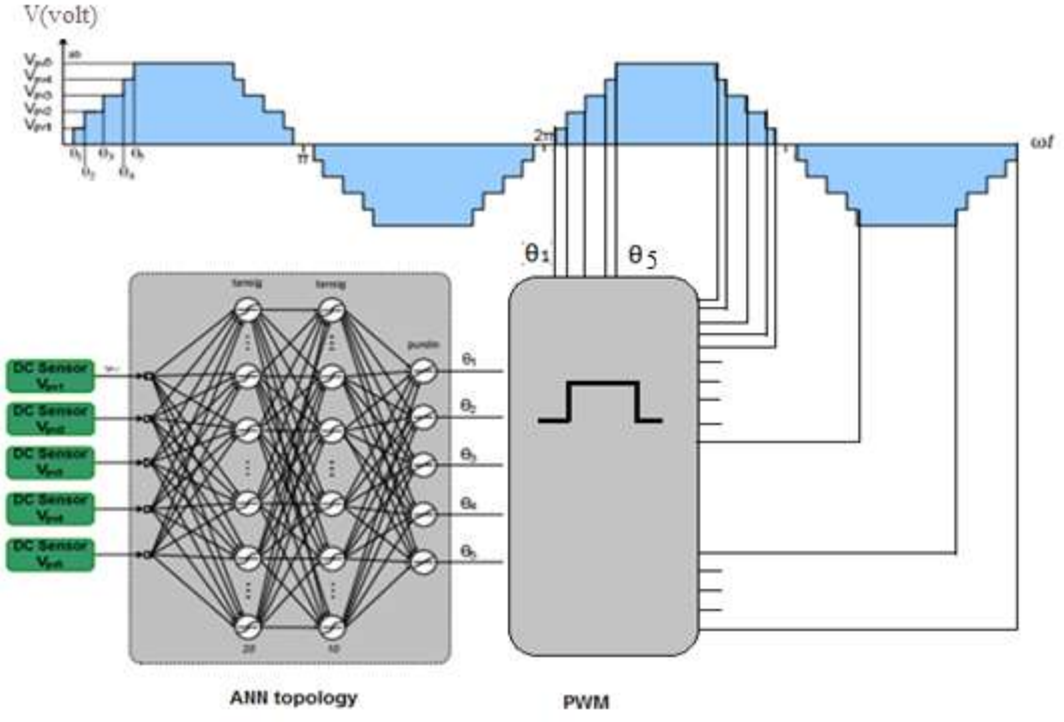

Fig (4.10) Pulse generation diagram

PWM is run in Matlab as shown in Fig (4.11), the output of PWM is shown in Fig (4.12)

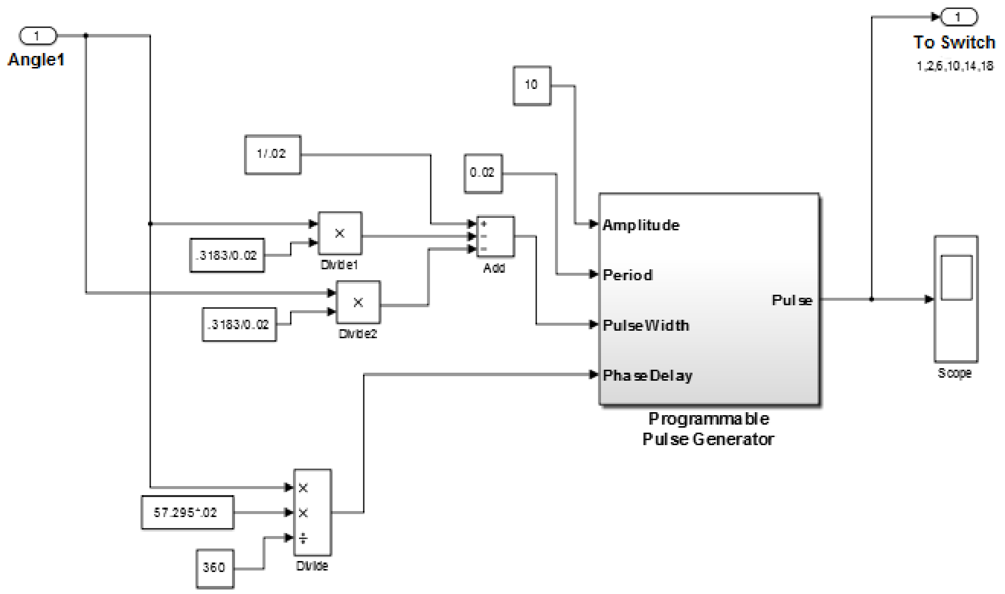

Fig (4.11) PWM diagram in Matlab Simulink

The conduction time, delay time, and switch status are shown in Table (4.2)

Table (4.2) Conduction time, delay time, and switch status

Angle Rad	Angle degree	Angle time
θ2	θ2*57.273	θ2*0.02/360
θ3	θ3*57.273	θ3*0.02/360
θ4	θ4*57.273	θ4*0.02/360
θ5	θ5*57.273	θ5*0.02/360
θ6	180-θ5	θ6*0.02/360
θ7	180-θ4	θ7*0.02/360
θ8	180-θ3	θ8*0.02/360
θ9	180-θ2	θ9*0.02/360
θ10	180-θ1	θ10*0.02/360
θ11	180+θ1	θ11*0.02/360
θ12	180+θ2	θ12*0.02/360
θ13	180+θ3	θ13*0.02/360
θ14	180+θ4	θ14*0.02/360
θ15	180+θ5	θ15*0.02/360
θ16	360-θ5	θ16*0.02/360
θ17	360-θ4	θ17*0.02/360
θ18	360-θ3	θ18*0.02/360
θ19	360-θ2	θ19*0.02/360
θ20	360-θ1	θ20*0.02/360

	0	Vdc1	Vdc2	Vdc3	Vdc4	Vdc5	Vdc4	Vdc3	Vdc2	Vdc1
angle	degree	θ2*57.273	θ3*57.273	θ4*57.273	θ5*57.273	180-θ5	180-θ4	180-θ3	180-θ2	180-θ1
time	θ1*0.02/360	θ2*0.02/360	θ3*0.02/360	θ4*0.02/360	θ5*0.02/360	θ6*0.02/360	θ7*0.02/360	θ8*0.02/360	θ9*0.02/360	θ10*0.02/36
switches										
1,2,6,10,14&18										
5										
9										
13										
17										
4,8,12,16,19&20										
15										
11										
7										
3										

0	-Vdc1	-Vdc2	-Vdc3	-Vdc4	-Vdc5	-Vdc4	-Vdc3	-Vdc2	-Vdc1	0
180+θ1	180+θ2	180+θ3	180+θ4	180+θ5	360-θ5	360-θ4	360-θ3	360-θ2	360-θ1	360
θ11*0.02/36	θ12*0.02/36	θ13*0.02/36	θ14*0.02/36	θ15*0.02/36	θ16*0.02/36	θ17*0.02/36	θ18*0.02/36	θ19*0.02/36	θ20*0.02/36	0.02

The output pulses of PWM are shown in Fig.(4.12)

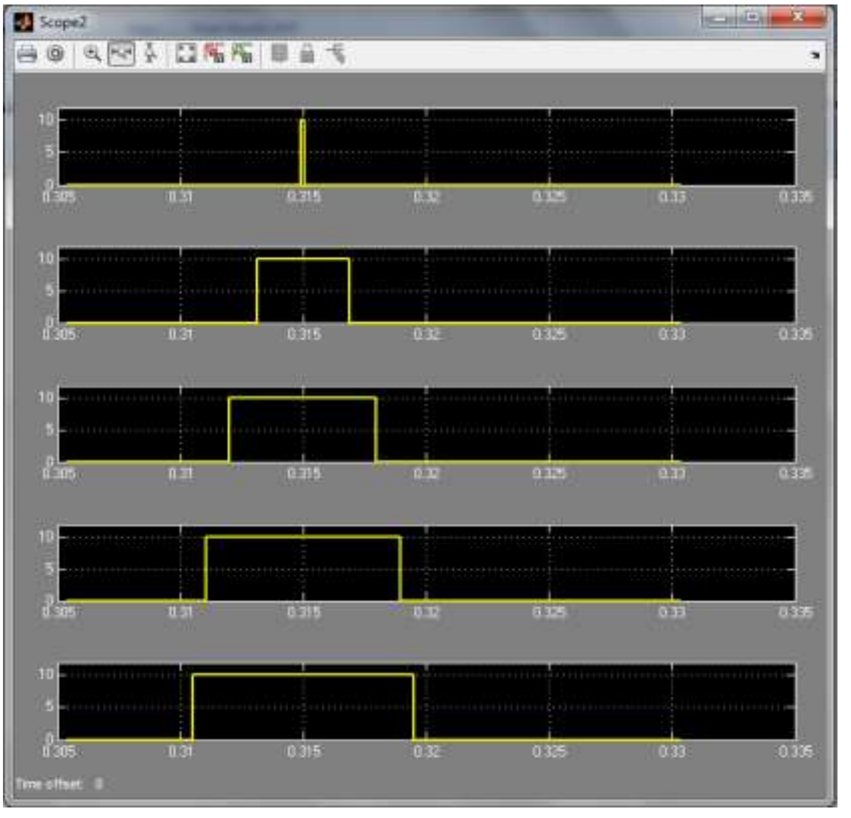

Fig (4.12a) generated pulses for first half cycle

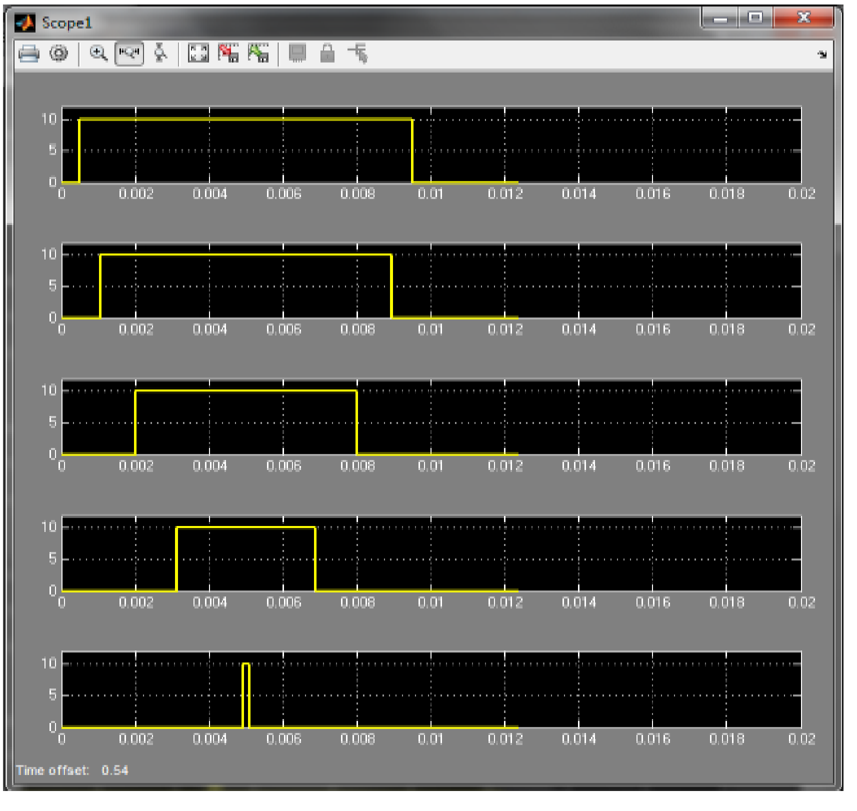

Fig (4.12b) generated pulses for second half cycle

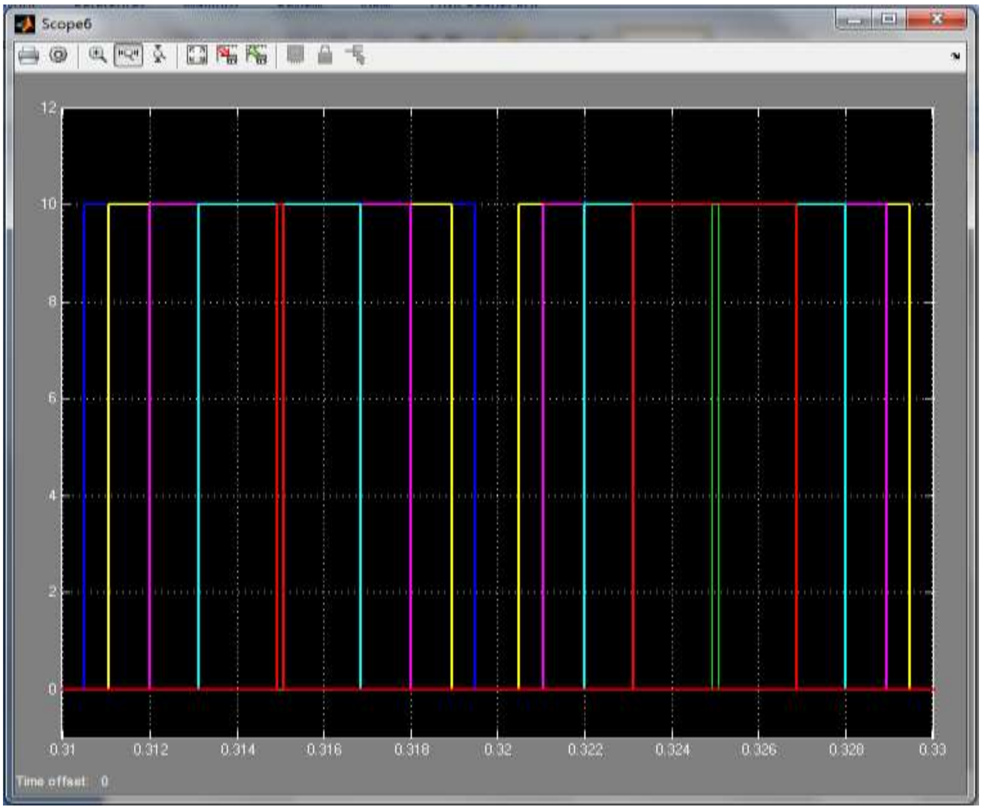

Fig (4.12c) projected pulses for one cycle

4.6. Chapter Summary

The output voltage formulas for balance and unbalance DC sources are derived using Fourier series, the nth harmonics equation (4.15-4.20) are used to build GA algorithm, the GA algorithm main principles, flow chart and parameters were illustrated. The GA algorithm running process and results were shown to verify its efficiency to find firing angles. Sample of output results are shown in table (4.1), due to large amount of results

The ANN principles, topology, and training were presented and explained, the number of hidden layer performance, and regression are shown in Fig.(4.6) and Fig.(4.7).

PWM is built and simulated in Matlab, the conduction time, delay time, and switch status

Are calculated in Table (4.3), its output pulses are verified as shown in Fig.(4.10)

Chapter Five
Results
&
Discussions

5.1. Results and Discussion

The proposed GA - ANN technique was tested on a single phase 11-level cascade H-bridge inverter using MATLAB R2013. In the proposed method, at first GA is used to solve the nonlinear equations and supply the desired switching angles.

Next, ANN is trained on the generated angle set produced by GA, which optimizes the switching angles of 11 level inverter so that 3_{rd}, 5_{th}, 7_{th}, and 9_{th} harmonics are minimized. The proposed model block of the tested MLI is shown in Fig.(5.1).

The Simulink model is shown in appendix 8

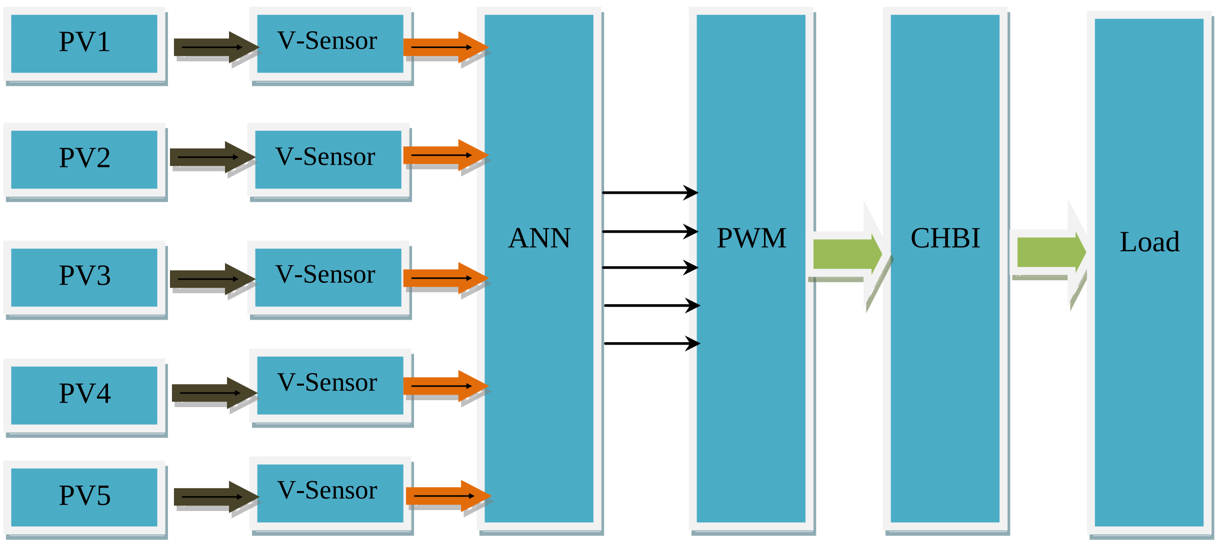

Fig.(5.1) proposed model block of the tested MLI

The output voltages and harmonics content depend on the generated switching angles produced by ANN, from the SIMLINK model is analyzed for different DC voltage levels, at first equal DC voltages are analyzed, Table (5.1) include a set of five equal DC sources, output RMS voltage, THD, and PV irradiation using 3Ω resistive load.

It is shown from table (5.1) that THD for equal voltage sources has a value of 9.3% whatever the DC voltage values are changed.

Table (5.1) Set of five equal DC sources, output RMS voltage, THD, and PV irradiation

irradiation (W/m2)	VDCs	Volt	Vout(rms)	R-Load	THD %
1000	v1	43.2	126.9	3	9.38%
1000	v2	43.2			
1000	v3	43.2			
1000	v4	43.2			
1000	v5	43.2			
800	v1	42.58	125.1	3	9.36%
800	v2	42.58			
800	v3	42.58			
800	v4	42.58			
800	v5	42.58			
500	v1	41.28	120.8	3	9.36%
500	v2	41.28			
500	v3	41.28			
500	v4	41.28			
500	v5	41.28			
100	v1	36.81	106.2	3	9.39%
100	v2	36.81			
100	v3	36.81			
100	v4	36.81			
100	v5	36.81			

The output voltage of the cascaded multilevel inverter at equal DC sources is shown in Fig.5.2, and the FFT analysis of output voltage is shown in Fig.5.3.

It is shown from Fig.5.2 that all the lower harmonics were minimized; the target harmonics (3rd, 5th, 7th and 9th) were in the percentage of 1.4% of fundamental voltage which mean they around zero values

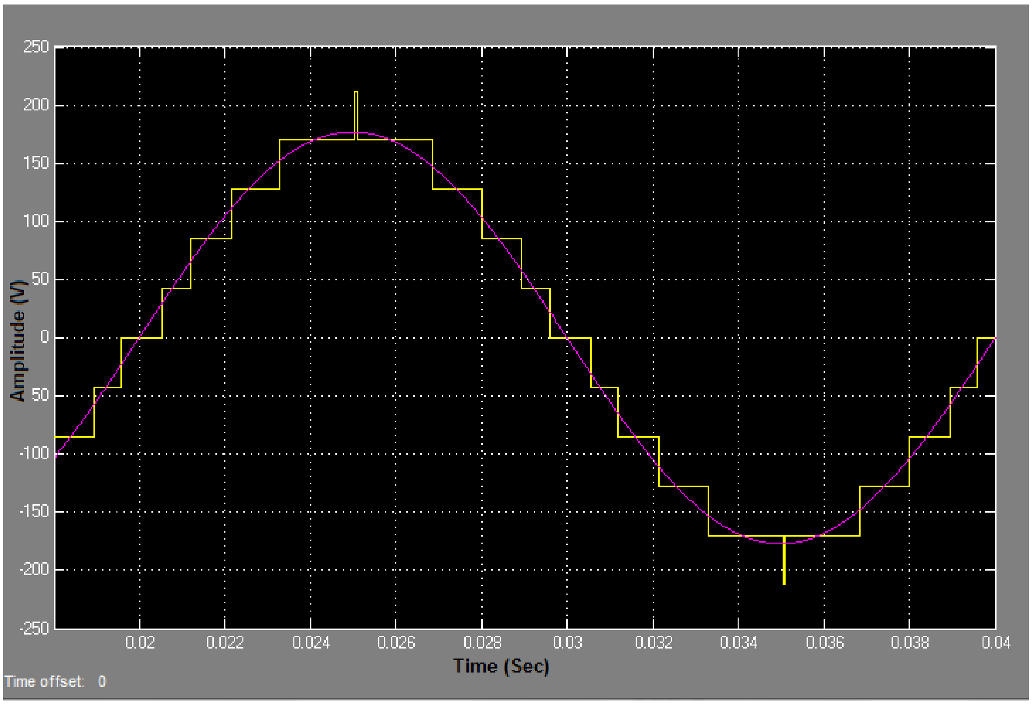

Fig.(5.2) The output voltage of the CMLI at equal DC sources

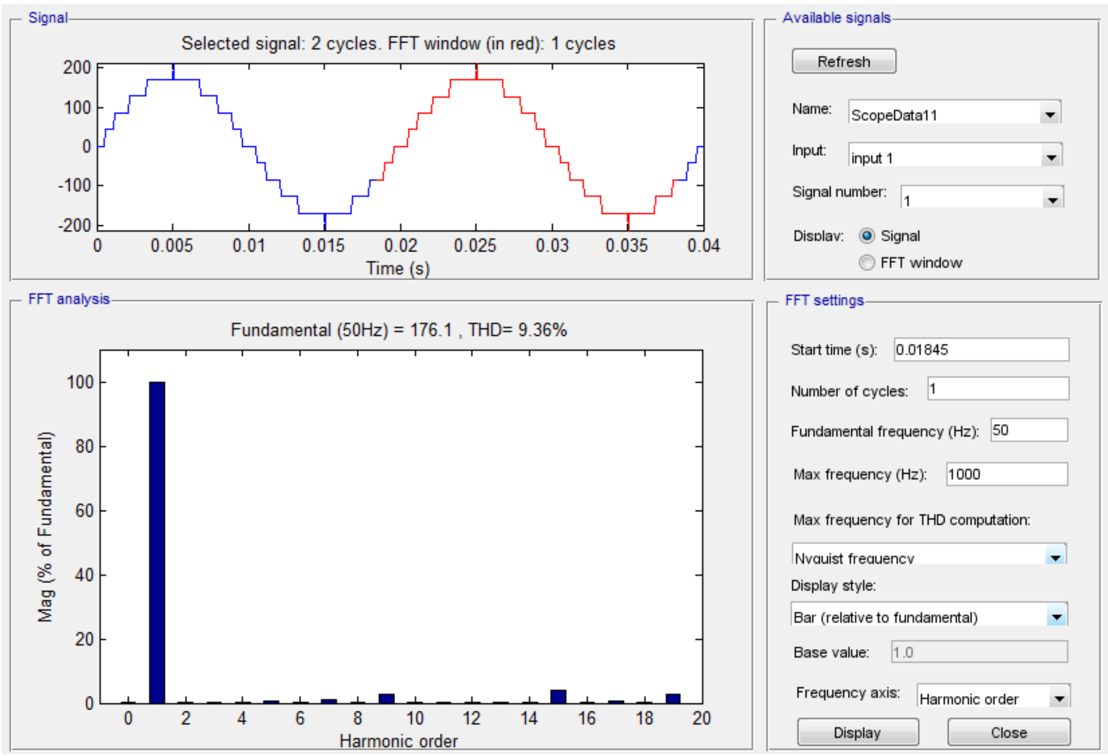

Fig.(5.3) FFT spectrum of CMLI output voltage at equal DC sources

Secondly unequal DC voltage sources are analyzed, Table (5.2) include a set of five unequal DC sources, output RMS voltage, THD, and PV irradiation using 3Ω resistive load

Table (5.2) a set of five unequal DC sources, output RMS voltage, THD, and PV irradiation

VDCs	Volt	Vout(rms)	R-Load	THD %
v1	36.81	**110.4**	**3**	**9.84%**
v2	36.81			
v3	36.81			
v4	41.28			
v5	41.28			
v1	36.81	**123.3**	**3**	**9.90%**
v2	36.81			
v3	43.2			
v4	43.2			
v5	43.2			
v1	36.81	**120.2**	**3**	**10.26%**
v2	36.81			
v3	41.28			
v4	42.58			
v5	43.2			
v1	24.54	**105.3**	**3**	**12.94%**
v2	24.54			
v3	27.52			
v4	35.46			
v5	35.97			

It is shown from table (5.2) that THD for unequal voltage sources increases when the DC sources variation increases, it starts from 9.84% when the variation equal to 4.47 [41.28-36.81] volts and increase to 12.94% when DC variation equal to 11.43 [35.97-24.54] volts.

The output voltage of the CMLI at unbalance DC sources is shown in Fig.(5.4) and Fig.(5.5) for DC variation of 4.47 and 11.43 respectively, the FFT analysis of output voltage of both cases are shown in Fig.5.6 and Fig.(5.7) respectively.

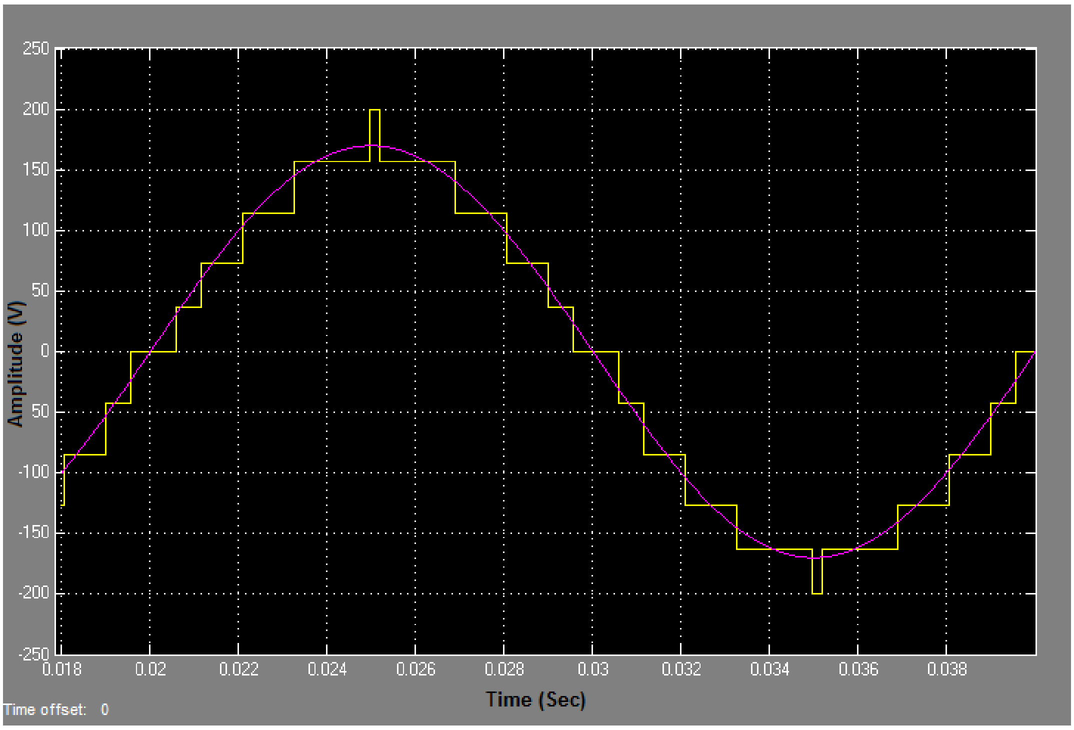

Fig.(5.4) The output voltage of the CMLI at unequal DC sources (DC variation = 4.47volts)

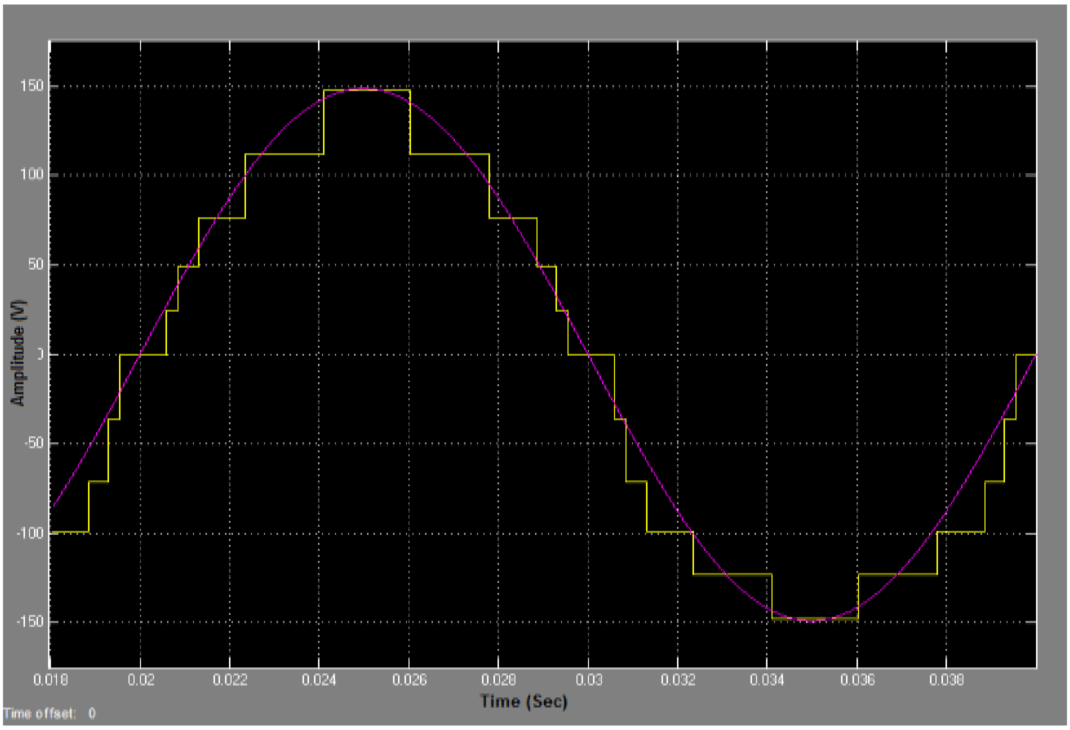

Fig.(5.5) The output voltage of the CMLI at unequal DC sources (DC variation = 11.43 volts)

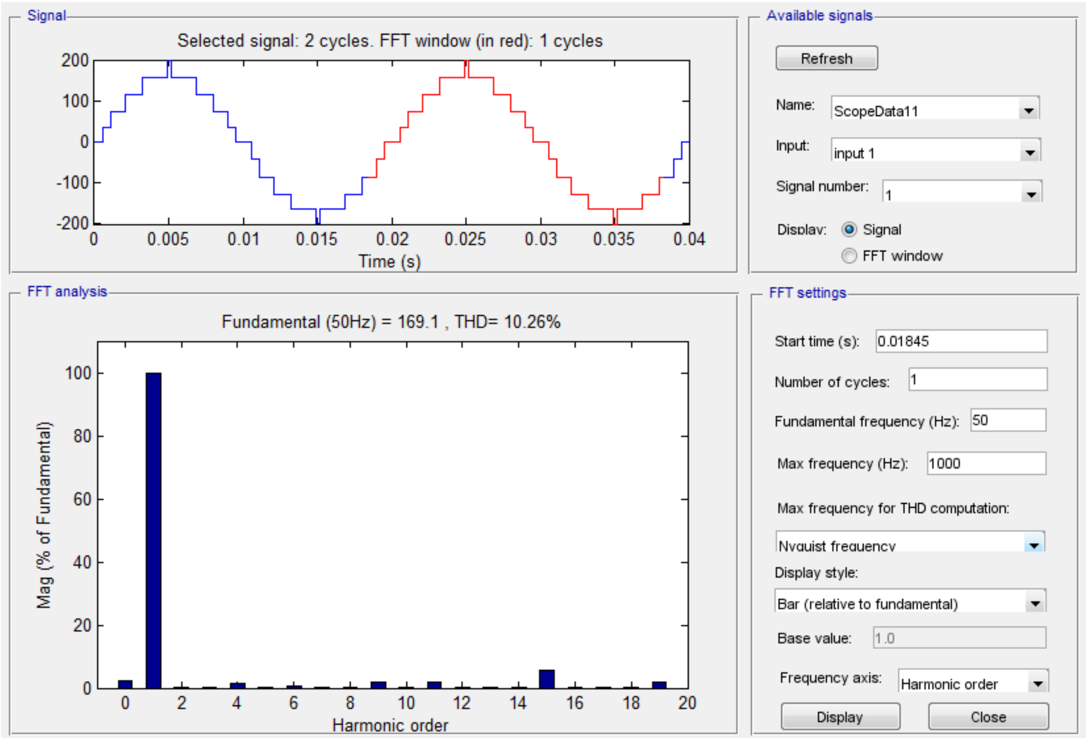

Fig.(5.6) FFT spectrum of CMLI output voltage at unequal DC sources (DC variation = 4.47 volts)

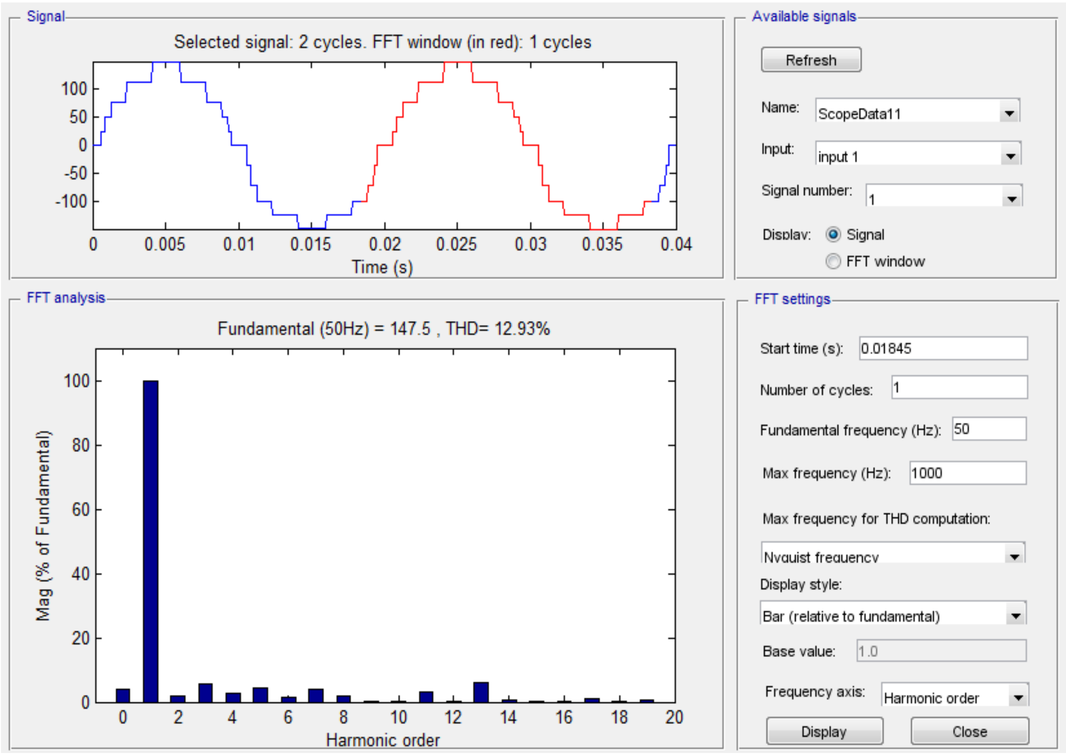

Fig.(5.7) FFT analysis of CMLI output voltage at unequal DC sources (DC variation = 11.43 volts)

It is shown from Fig.5.6 and Fig.5.7 that the target harmonics (3rd, 5th, 7th and 9th) were in the percentage of 1.1% to 3.7% of fundamental voltage at maximum DC variation

5.2. Genetic Algorithm Parameters Tuning

The main problem with GA that the population size and generations must be set each trial of solution, by observing fitting procedure and fitness of each individual it can be determined if setting parameters are right and GA doesn't fall in local minima, or parameters have to be reset again, and since there are tens of sets of input voltage, too much time is consumed, the difference between two cases are shown in Fig.5.8 and Fig. 5.9, for best setting of parameters which produce switching angles (0.1646, 0.4638, 0.8826, 1.5110, 1.5708)

But when the parameters are set wrong as shown in Fig.5.10, and Fig.5.11, the switching angles produced are (0.1648, 0.4642, 0.8837, 1.5401, 1.5429)

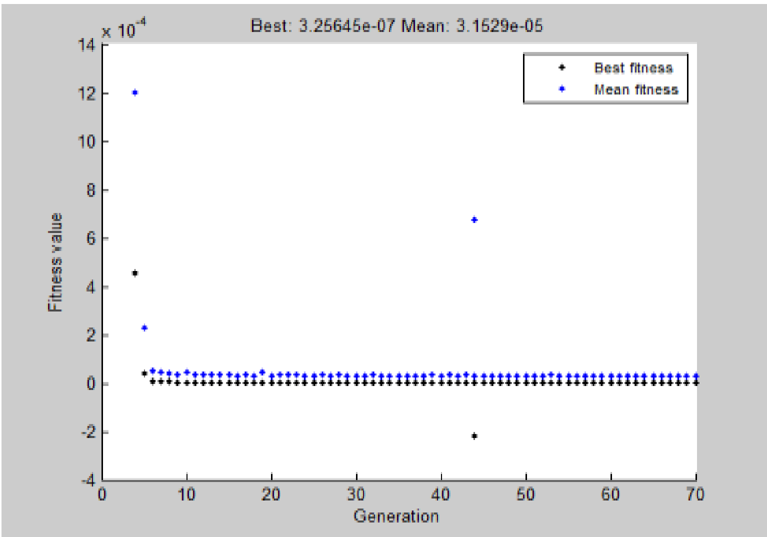

Fig.(5.8) Fitness when parameters are set right

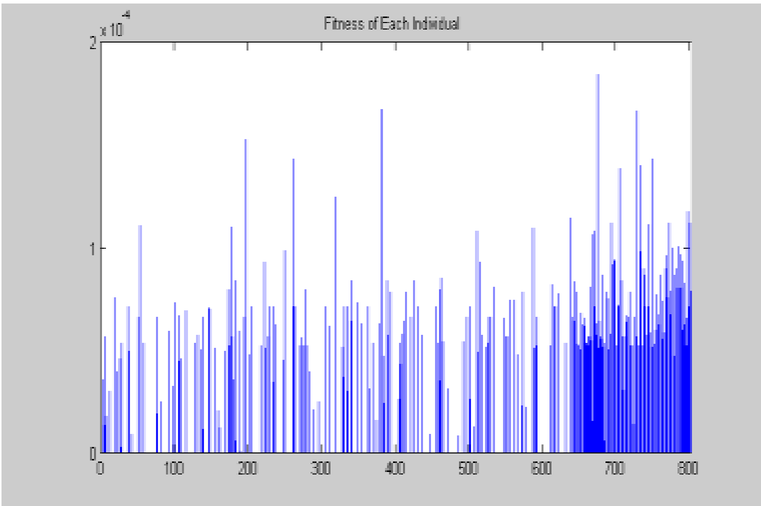

Fig.(5.9) Fitness if each individual when parameters are set right

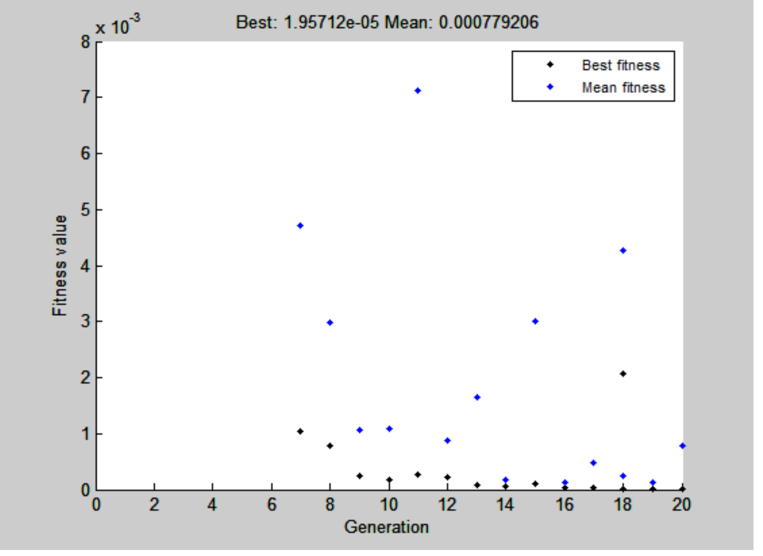

Fig.(5.10) Fitness when parameters are set wrong

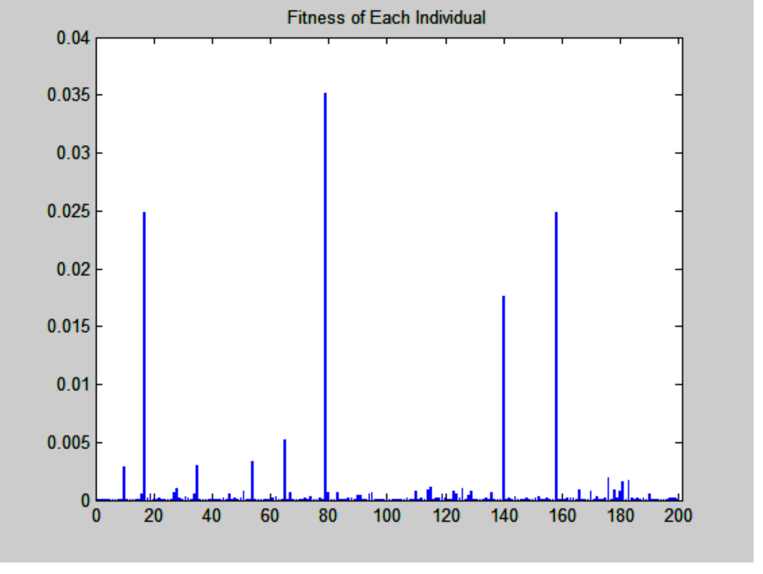

Fig.(5.11) Fitness if each individual when parameters are set wrong

5.3. Neural Network Training Setting

Many parameters and algorithms control the ANN training accuracy, at first choosing number of hidden layers and their activation functions, secondly number of neurons in each hidden layer, thirdly the training algorithm function and its special parameters since the default parameters can't work with random relation between inputs and outputs, all these parameters must be chosen exactly to get high training regression,

An example of miss choosing wrong algorithm will result with bad performance as shown in Fig.(5.12), while choosing right algorithm will result good performance as shown in Fig.(5.13).

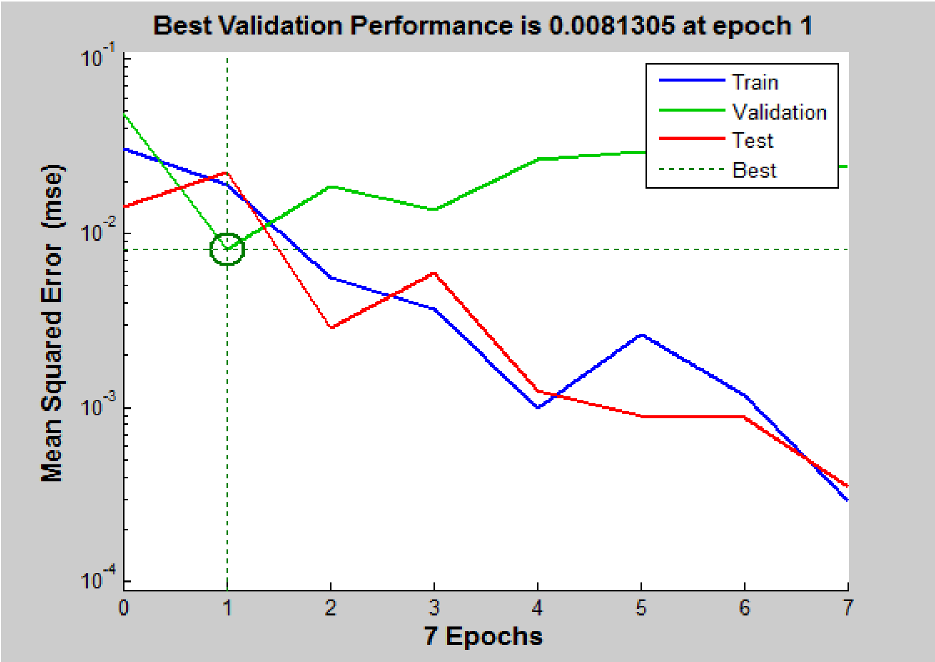

Fig.(5.12) ANN training using wrong algorithm

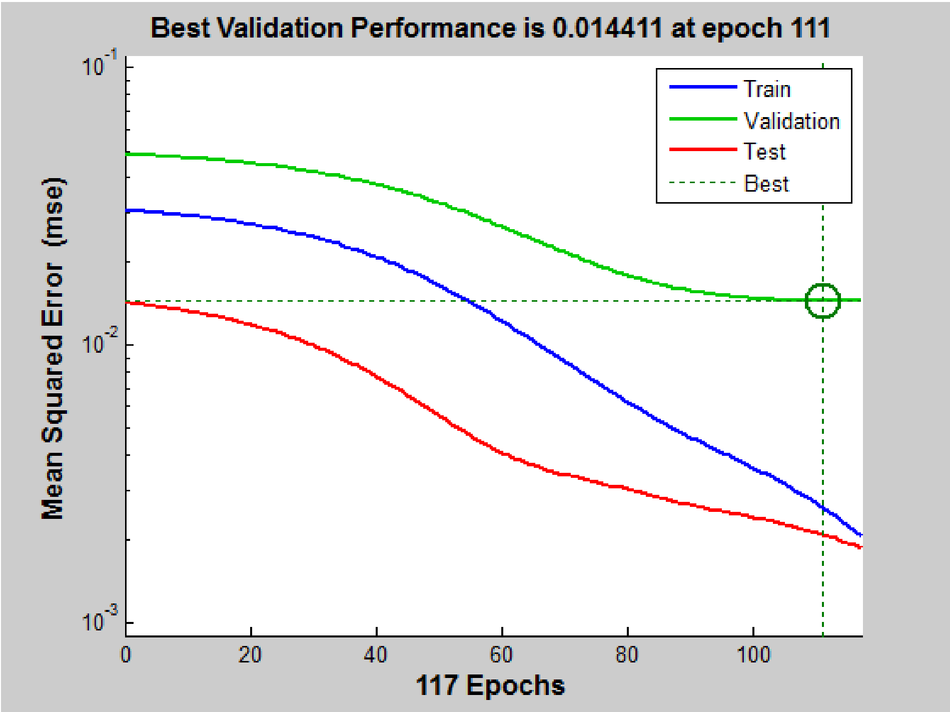

Fig.(5.13) ANN training using right algorithm

Chapter Six
Conclusion

6.1. Comparison

Many algorithms are used to solve SHE equations for 11 level CHB MLI, we browse here the results were got by researchers and compare with this research technique, tables (6.1, 6.2, and 6.3) researchers uses their techniques to solve SHE equations and apply to pulse generators directly and don't use ANN, so the THD must be low since ANN can't give exact results.

Table (6.4) researcher used Newton Raphson method to solve the equations and then trained ANN using BPA and got 9.79% THD for equal DC sources, however our proposed technique (GA and ANN) in table (6.5) gives 9.38% THD at equal DC sources.

Table 6.1: Modified Newton–Raphson and Pattern Generation Methods

According to Ref [28]				
Modified Newton–Raphson and Pattern Generation Methods/ ANN is not used				
V_{DC} (v)	Angle (rad)	Angle (degree)	THD	V_{rms}
35	0.622	35.62	9.8%	94.3
35	0.8333	47.726		
35	1.049	60.079		
35	1.313	75.199		
35	1.561	89.403		

Table 6.2: Newton–Raphson Method

According to Ref [29]				
Newton–Raphson Method /ANN is not used				
V_{DC} (p.u)	Angle (rad)	Angle (degree)	THD	V_{rms}
1	0.137	7.859	8.56%	………
1	0.338	19.372		
1	0.518	29.652		
1	0.833	47.680		
1	1.104	63.212		
V_{DC} (p.u)	angle	degree	THD	V_{rms}
1.1	0.155	8.894	8.2%	…………
1.05	0.354	20.250		
1	0.564	32.310		
0.95	0.878	50.260		
0.9	1.112	63.690		

Table 6.3: Different Techniques

According to Ref [30]							
(PSO/ABCA/FA)/ANN is not used							
Technique	MI	θ1	θ2	θ3	θ4	θ5	THD%
PSO	0.47	37.71	52.81	68.2	86.25	89.4	44.98
ABCA		12.79	35.79	58.99	87.61	90	14.83
FA		12.59	34.85	58.59	88.98	89.98	14.56
PSO	0.7	16.73	36.03	56.24	88.37	88.37	21.39
ABCA		11.98	24.17	38.56	59.49	59.49	13.75
FA (proposed)		3.08	15.33	33.74	84.24	84.24	12.88

Table 6.4: Newton–Raphson Methods with ANN

According to Ref [31]				
Newton Raphson method /ANN is trained using BPA				
V_{DC} (p.u)	Angle (rad)	Angle (degree)	THD	Vrms
1	0.067	7.859	9.79%	65.4
1	0.222	19.372		
1	0.425	29.652		
1	0.662	47.680		
1	0.963	63.212		

Table 6.5: Proposed Technique

Proposed Technique					
Genetic Algorithm method /ANN is feed forward trained					
	VDC (v)	Angle (rad)	Angle (degree)	THD	Vrms
Equal DC Sources	43.2	0.151	8.660	9.38%	126.9
	43.2	0.366	20.973		
	43.2	0.656	37.594		
	43.2	1.028	58.888		
	43.2	1.550	88.767		
Unequal DC Sources	36.81	0.149	8.56	10.26%	110.4
	36.81	0.377	21.601		
	36.81	0.666	38.131		
	41.28	1.033	59.154		
	41.28	1.549	88.742		
Proposed Technique					

Genetic Algorithm method /ANN is feed forward trained					
	VDC (v)	Angle (rad)	Angle (degree)	THD	Vrms
Unequal DC Sources	24.54	0.153	8.772	12.94%	105.3
	24.54	0.246	14.084		
	27.52	0.318	18.221		
	35.46	0.645	36.94		
	35.97	1.051	60.202		

6.2. The impact of ANN at shading conditions:

Due to shading conditions, significant change occur in the PV current and voltage, which is equivalent to change in the actual radiations strikes the panel surface. The following descriptions, present a brief comparison for the generated values of MLI firing angles without and with applying ANN comparing with another GA algorithms.

ANN can reduce THD under shading conditions, since it can amend the firing angles of MLI, if a set of equal DC sources firing angles are fed to MLI and considered as optimum to minimize THD, they will be unuseful when shading happens since they are a solution of one case not all cases, but ANN can supply MLI with best set of firing angles for all cases within training range.

As an example GA best firing angles for equal DC are (8.161, 20.251, 37.284, 57,759, 89.689) when supplied directly to PWM, the output voltage THD is 9.55% and RMS= 126.7 volt. **But when DC sources varies due to shading the THD will increase depend on DC** variation while ANN can control the THD to be minimum as possible by supplying the MLI with correct (adjusted) firing angle.

Table (6.6) compares between output THD and RMS value without and with using ANN when DC sources are equal, and table (6.7) compares between output THD and RMS value without and with using ANN when DC sources are unequal.

Table 6.6 Set of five equal DC sources, output RMS voltage, THD, and PV irradiation without and with ANN

Control strategy	Without ANN				With ANN		
Irradiation (W/m^2)	VDC (volt)	GA firing angles	GA THD	GA RMS (volt)	ANN firing angles	ANN THD	ANN RMS (volt)
1000		8.659			8.161		
1000		20.973			20.251		
1000	43.2	37.594	9.55%	126.7	37.284	9.43%	127
1000		58.888			57.759		
1000		88.767			89.689		
1000							

The obtained results of table (6.6) are shown in Fig.(6.1) and Fig.(6.2)

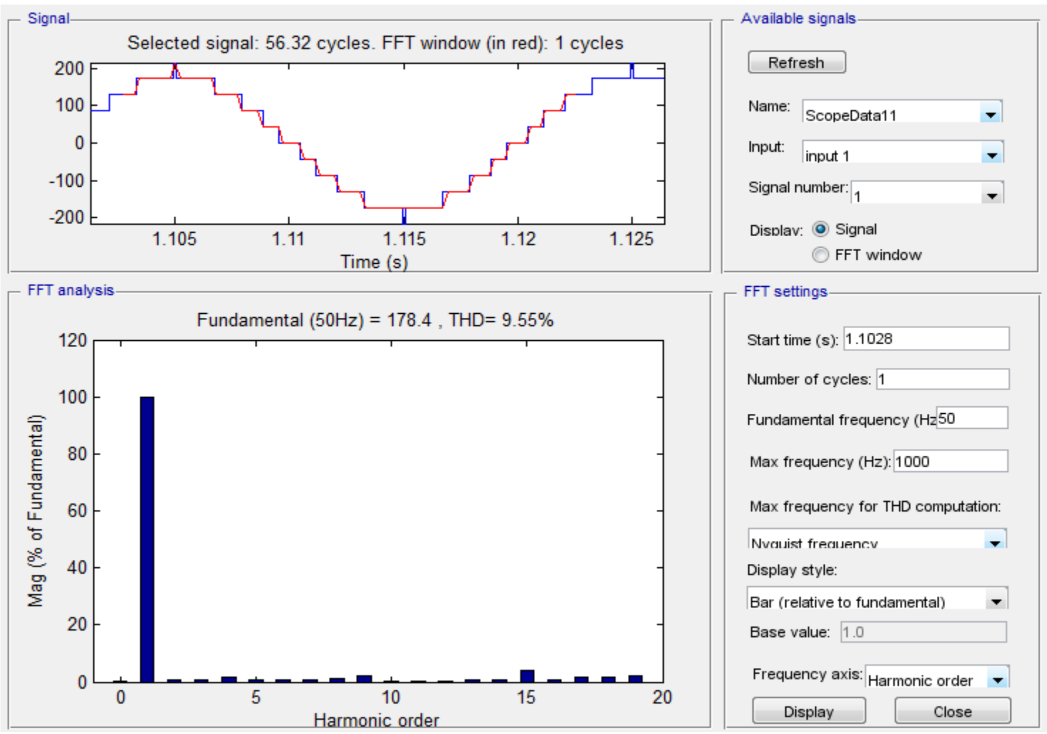

Figure (6.1) THD results from GA firing angles

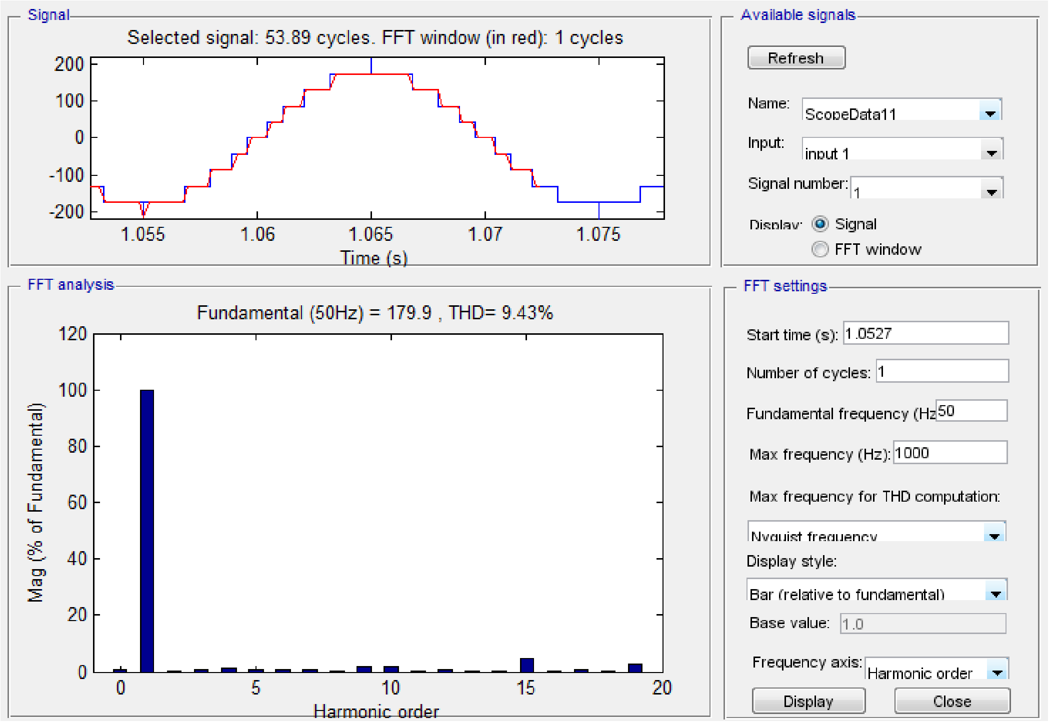

Figure (6.2) THD results from ANN firing angles

Table (6.7) Set of five unequal DC sources, output RMS voltage, THD, and PV irradiation without and with ANN

Control strategy							Without ANN (GA)			With ANN		
Irradiation (W/m^2)						VDC (volt)	GA firing angles	GA THD	GA RMS (volt)	ANN firing angles	ANN THD	ANN RMS (volt)
1000	**1000**	**1000**	**1000**	**1000**	**1000**	43.2	8.659			7.903		
500	**1000**	**1000**	**1000**	**1000**	**1000**	42.88	20.97			19.93		
500	**500**	**1000**	**1000**	**1000**	**1000**	42.56	37.59			36.31		
500	**500**	**500**	**500**	**500**	**500**	41.28	58.88	9.95%	121.5	58.07	8.85%	122.1
0	**1000**	**1000**	**1000**	**1000**	**1000**	35.97	88.76			91.57		
400	**400**	**400**	**400**	**400**	**400**	40.66	8.659			8.596		
200	**200**	**200**	**200**	**200**	**200**	38.73	20.97			18.78		
800	**800**	**800**	**800**	**800**	**800**	42.58	37.59			34.70		
1000	**1000**	**1000**	**1000**	**1000**	**1000**	43.2	58.88	9.90%	119.2	57.73	9.44%	120.7
100	**100**	**100**	**100**	**100**	**100**	36.81	88.76			90.94		
0	**400**	**400**	**400**	**400**	**400**	33.86	8.659			9.157		
0	**200**	**200**	**200**	**200**	**200**	32.25	20.97			19.35		
0	**800**	**800**	**800**	**800**	**800**	35.46	37.59			35.56		
0	**1000**	**1000**	**1000**	**1000**	**1000**	35.97	58.88	10.4%	104.1	58.99	9.89%	100
0	**100**	**100**	**100**	**100**	**100**	30.65	88.76			88.77		
0	**0**	**400**	**400**	**400**	**400**	27.1	8.659			8.590		
0	**0**	**200**	**200**	**200**	**200**	25.82	20.97			20.50		
0	**0**	**800**	**800**	**800**	**800**	28.39	37.59			28.80		
0	**0**	**1000**	**1000**	**1000**	**1000**	28.8	58.88	9.93%	79.48	48.73	9.37%	95.08
0	**0**	**100**	**100**	**100**	**100**	24.54	88.76			63.45		

The obtained results of first two cases illustrated in table (6.7) are shown in Fig.(6.3) to Fig.(6.6)

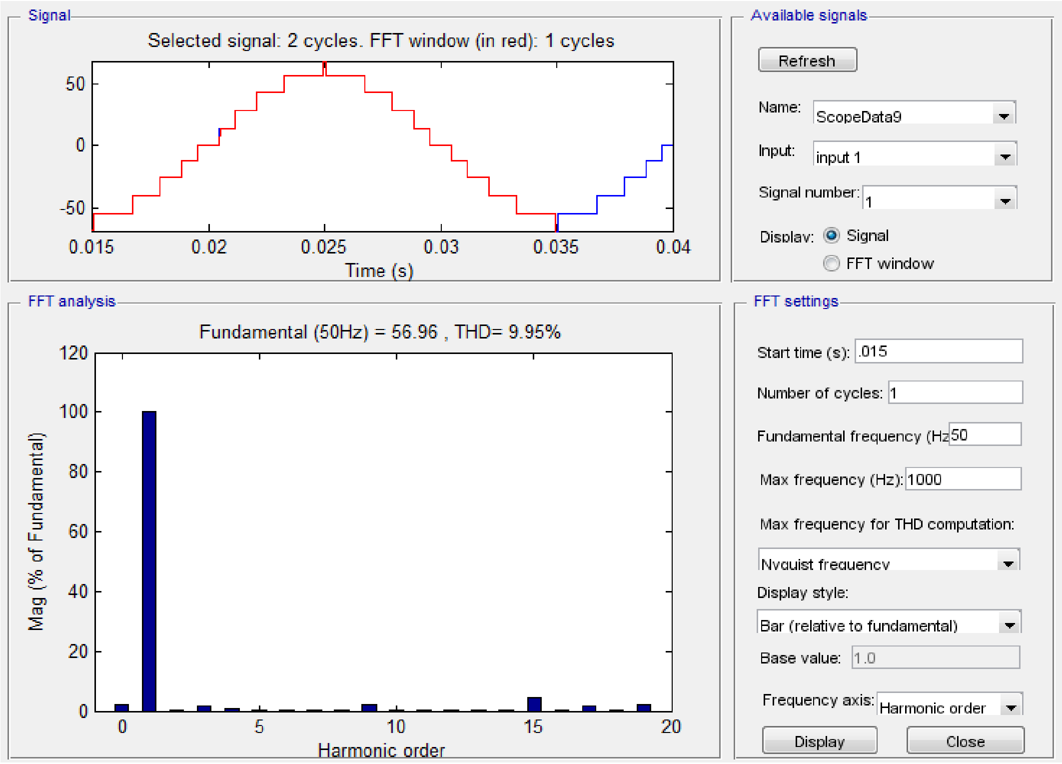

Fig.(6.3) THD results from GA when DC sources are unequal

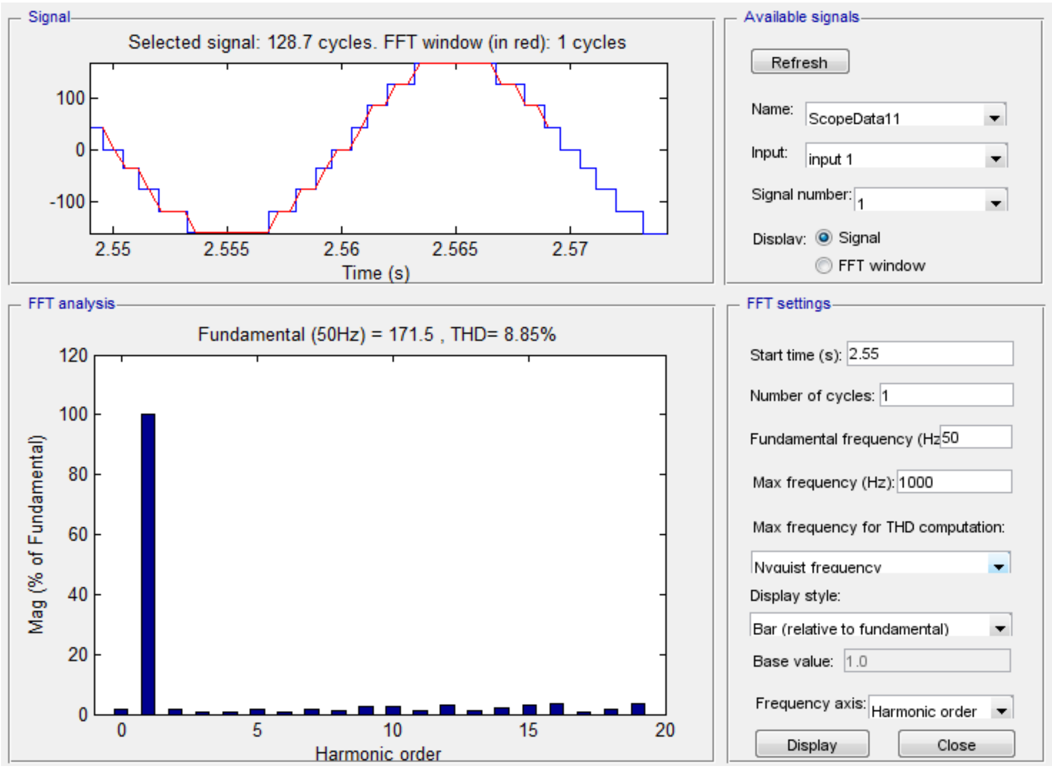

Fig.(6.4)THD results from ANN when DC sources are unequal

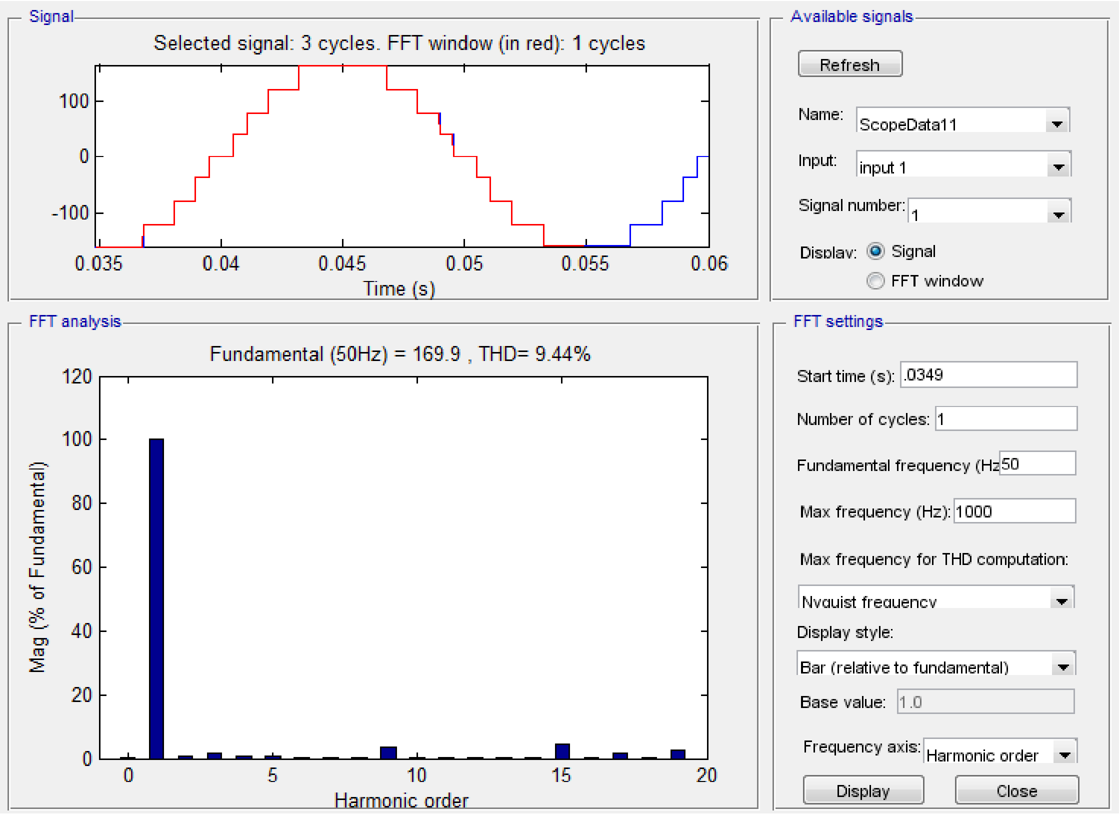

Fig.(6.5)THD results from ANN when DC sources are unequal

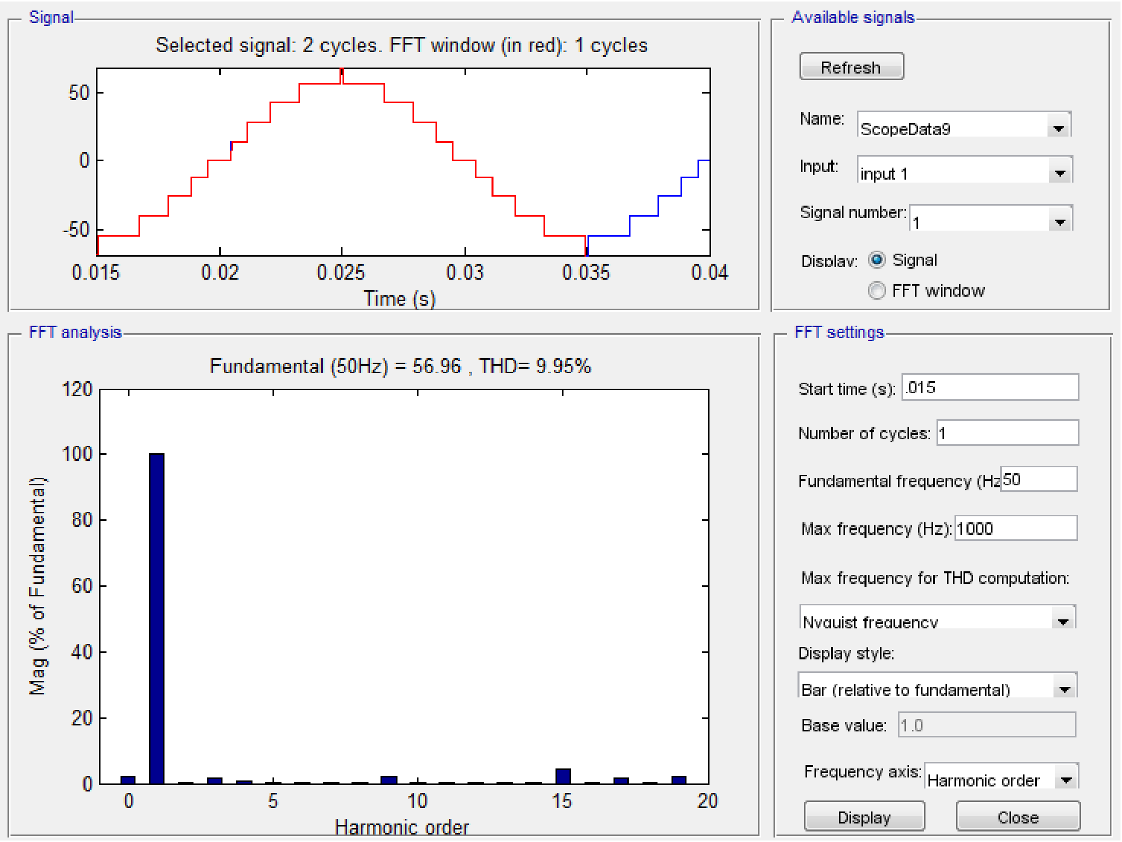

Fig.(6.6)THD results from GA when DC sources are unequal

6.3 Conclusion

The following conclusions can be stated:

1. By applying GA nonlinear equations of SHE were successfully resolved, GA algorithm must run many times to get the best solution, you can note that through value of generated angles.
2. Main parameters such as Population and generation size, operator and fitness function have to be set again when the input DC voltage are changed . tuning crossover a bit little speed up the run
3. A feed forward (ANN) proves that it can generate the desired switching angles however the voltage level changed by keeping the fundamental while eliminating the target harmonics.
4. GA and ANN technique achieve minimum THD for both equal and unequal DC sources, and can be applied for any kind of level inverter. According to our calculations to find THD for fixed DC sources we obtain 9.38%, while in previous researches used ANN the best THD obtained was 9.8%, and for variable DC sources we obtained 9.84% THD

6.4. Recommendation

For enhancing the quality of generated pulse patterns and reducing the calculation time, we do recommend the following:

1. Use GA to solve the nonlinear equations, it is useful technique to achieve exact or approximate solution when analytical methods can't help you.
2. Set the GA parameters and active function exactly to get best results.
3. Choose ANN topology that fit your data complexity, number of hidden layers and activation function depend on relation between input and output data.
4. Choose a set of input voltages that not vary more than 15%, you will get better result and facilitate ANN training
5. Use three phase MLI so you can eliminate the 11^{th} and 13^{th} harmonics, 3^{rd} and 9^{th} harmonics cancelled automatically, which decreases the THD.

6.5. Future Work

For completing the already started work, we do advise:

1. Controlling the ANN bias to fit the load variation, so the switching angles can be adjusted depends on DC inputs and load variation.
2. Studying the running time delay of ANN and its effect on THD
3. Using ANN with maximum power point tacking to achieve maximum output power.
4. Apply the results practically for comparison between simulation and experimental results

References

[1] Gilbert M. Masters Copyright, 2004 by John Wiley & Sons, Inc., Hoboken, New Jersey. All rights reserved, Published by John Wiley & Sons, Inc., Hoboken, New Jersey. Published simultaneously in Canada

[2] Muhammad H. Rashid "Power Electronics Devices, Circuits, and Applications" fourth edition, pp 441-466

[3] J. Rodriguez, J. Lai, F. Z. Peng, "Multilevel inverters: a survey of topologies, control and applications," IEEE Transactions on Industrial Electronics, vol. 49, no. 4, pp.724-738, Aug. 2002.

[4] A. Pandey, B. Singh, B. N. Singh, A. Chandra, K. Al-Haddad, D. P. Kothari, "A review of multilevel power converters," Institute of Engineers Journal (India) , pp.220-231, vol. 86, March 2006.

[5] S. Kouro,M. Malinowski, K. Gopakumar, J. Pou, L. G. Franquelo, B. Wu, J.Rodriguez, M. A. Perez, J. I. Leon, "Recent advances and industrial applications of multilevel converters, " IEEE Transactions on Industrial Electronics, vol. 57, no. 8, pp. 2553-2580, Aug. 2010.

[6] R. Rangarajan, F. E. Villaseca, "A switching scheme for multilevel converters with non-equal DC sources, " 39th North American Power Symposium, pp. 308-313, Sept.2007.

[7] B. Ozpineci, L. M. Tolbert, J. N. Chiasson, "Harmonic optimization of multilevel converters using genetic algorithms," IEEE Power Electronics Letters, vol. 3, no. 3, pp. 92-95, Sept. 2005.

[8] J. N. Chiasson, L. M. Tolbert, K. J. McKenzie, Z. Du, "A unified approach to solving the harmonic elimination equations in multilevel converters," IEEE Transactions onPower Electronics, vol. 19, no. 2, pp. 478-490, Mar. 2004.

[9] J. N. Chiasson, L. M. Tolbert, K. J. McKenzie, Z. Du, "Elimination of harmonics in a multilevel converter using the theory of symmetric polynomials and resultants," IEEE Transactions on Control Systems Technology, vol. 13, no. 2, pp. 216-223, March 2005.

[10] Z. Du, L. M. Tolbert, J. N. Chiasson, H. Li, "Low switching frequency active harmonic elimination in multilevel converters with unequal DC voltages," Annual Meeting of the IEEE Industry Applications Society, pp. 92-98, Oct. 2005.

[11] Z. Du, L. M. Tolbert, J. N. Chiasson, "Active harmonic elimination for multilevel converters," IEEE Transactions on Power Electronics, vol. 21, no. 2, pp. 459-469,March 2006.

[12] D. Ahmadi, Jin Wang, "Selective harmonic elimination for multilevel inverters with unbalanced DC inputs," IEEE Vehicle Power and Propulsion Conference, pp. 773-778, Sept. 2009.128

[13] M. Dahidah, V. G. Agelidis, “Selective harmonic elimination multilevel converter control with variant DC sources,” IEEE Conference on Industrial Electronics and Applications, pp. 3351-3356, May 2009.

[14] L. G. Franquelo, J. Rodriguez, J. I. Leon, S. Kouro, R. Portillo, M. A. M. Prats, “The age of multilevel converters arrives,” IEEE Industrial Electronics Magazine, vol. 2,no. 2, pp. 28-39, June 2008

[15] Xue, Y. Ge, B, and Peng. F. Z, "Reliability, efficiency, and cost comparisons of MW-scale photovoltaic inverters", IEEE Energy Conversion Congress and Exposition (ECCE),2012

[16] M. S. A. Dahidah, V. G. Agelidis, “Selective harmonic elimination PWM control for cascaded multilevel voltage source converters: A generalized formula,” IEEE Transactions on Power Electronics, vol. 23, no. 4, pp. 1620-1630, July 2008

[17]. F. J. T. Filho, L. M. Tolbert, Y. Cao, B. Ozpineci, ―Real time selective harmonic minimization for multilevel inverters connected to solar panels using artificial neural network angle generation, IEEE Energy Conversion Congress and Exposition, pp. 594-598, Sept. 2010.

[18] M. Srinivas, L. M. Patnaik, “Genetic algorithms: a survey, ” IEEE Computer Society Press., vol. 27, no. 6, pp. 17-26, Jun 1994.

[19] D. E. Goldberg, Genetic Algorithms in Search, Optimization, and Machine Learning. MA: Addison-Wesley, 1989.

[20] K.F. Man, K.S. Tang, S. Kwong, “Genetic algorithms: concepts and applications [in engineering design],” IEEE Transactions on Industrial Electronics, vol.43, no.5, pp.519-534, Oct 1996.

[21] C. R. Houck, J. A. Joines and M. G. Kay, “A genetic algorithm for function optimization: A Matlab implementation,” Technical Report NCSU-IE-TR-95-09, North Carolina State University, Raleigh, NC (1995).

[22] J. J. Hopfield, “Artificial neural networks,” IEEE Circuits and Devices Magazine, vol. 4, no. 5, pp. 3-10, Sep. 1988.129

[23] R. Aggarwal, Y. Song, “Artificial neural networks in power systems II: types of artificial neural networks,” Power Engineering Journal, vol. 12, no. 1, pp. 41-47, Feb. 1998.

[24] R. Aggarwal, Y. Song, “Artificial neural networks in power systems I: general introduction to neural computing,” Power Engineering Journal, vol. 11, no. 3, pp. 129-134, Jun. 1997.

[25] M. J. Willis, C. Di Massimo, G. A. Montague, M. T. Tham, A. J. Morris, “Artificial neural networks in process engineering,” IEE Procedings in Control Theory and Applications, vol. 138, no. 3, pp. 256-266, May 1991.

[26] A. K. Jain, Jianchang Mao, K. M. Mohiuddin, “Artificial neural networks: a tutorial,” Computer , vol. 29, no. 3, pp. 31-44, Mar 1996.

[27] Mohammed Al-Hitmi, Salman Ahmad, Atif Iqbal , Sanjeevikumar Padmanaban and Imtiaz Ashraf." Selective Harmonic Elimination in a Wide Modulation Range Using Modified Newton–Raphson and Pattern Generation Methods for a Multilevel Inverter, Energies 2018, 11, 458

[28] V.Joshi Manohar, M.Trinad, K.Venkata Ramana, "Comparative Analysis of NR and TBLO Algorithms in Control of Cascaded MLI at Low Switching Frequency, Elsevier B.V, 2016, 1877-0509

[29] A. K. Jain, Jianchang Mao, K. M. Mohiuddin, “Artificial neural networks: a tutorial,” Computer , vol. 29, no. 3, pp. 31-44, Mar 1996.

[30] Dr. R. K. Singh," Artificial Neural Network Based Harmonic Optimization of Multilevel Inverter to Reduce THD", Proc. of the Intl. Conf. on Advances in Computer, Electronics and Electrical Engineering Editor, 2012, ISBN: 978-981-07-1847-3

[31] Sihem. Ghoudelbourk, D. Dib, B. Meghni, and M. Zouli," Selective harmonic elimination strategy in eleven level inverter for PV system with unbalanced DC sources", (2017) AIP Conference Proceedings 1814, 020008

[32] A. Zama , S. Ait Mansour , D. Frey, A. Benchaib , S. Bacha, and B. Luscan," A Comparative Assessment of Different Balancing Control Algorithms for Modular Multilevel Converter (MMC)", Super Grid Institute SAS, 130 Leon Blum, BP 1321, 69611 Villeurbanne, France Université Grenoble Alpes-Laboratoire G2Elab, 21 avenue des Martyrs, 38031 Grenoble, France.

Appendices

Appendix (1): GA Fitness function

```
Function y = my Fitness(x)


y=(1/120)*sqrt(((.300105*(39*cos(3*x(1))+39*cos(3*x(2))+39*cos(3*x(3))+39*cos(3*x(4))+39*
cos(3*x(5)))))^2

+

(.18*((39*cos(5*x(1))+39*cos(5*x(2))+39*cos(5*x(3))+39*cos(5*x(4))+39*cos(5*x(5)))))^2

+

(.128*((39*cos(7*x(1))+39*cos(7*x(2))+39*cos(7*x(3))+39*cos(7*x(4))+39*cos(7*x(5)))))^2 +

(.1*((39*cos(9*x(1))+39*cos(9*x(2))+39*cos(9*x(3))+39*cos(9*x(4))+39*cos(9*x(5)))))^2);


End
```

Appendix (2): GA constraints function

```
Function[c,c_eq] = my Constraints (x)

 c = [(.903*(39*cos(x(1))+39*cos(x(2))+39*cos(x(3))+39*cos(x(4))+39*cos(x(5))) - 120);.

0.30010*(39*cos(3*x(1))+39*cos(3*x(2))+39*cos(3*x(3))+39*cos(3*x(4))+39*cos(3*x(5)));.

0.18*(39*cos(5*x(1))+39*cos(5*x(2))+39*cos(5*x(3))+39*cos(5*x(4))+39*cos(5*x(5)));.

0.1286*(39*cos(7*x(1))+39*cos(7*x(2))+39*cos(7*x(3))+39*cos(7*x(4))+39*cos(7*x(5)));.

0.1*(39*cos(9*x(1))+39*cos(9*x(2))+39*cos(9*x(3))+39*cos(9*x(4))+39*cos(9*x(5)))];

c_eq =[ ];

End
```

Appendix (3): GA Main Function

```
ObjFcn = @myFitness;

nvars = 5;

A = [1 -1 0 0 0;0 1 -1 0 0;0 0 1 -1 0;0 0 0 1 -1;0 0 0 0 0];

b = [0;0;0;0;0];

LB = [0 0 0 0 0];

UB (1:5)= pi/2;

ConsFcn = @myConstraints;

 options = gaoptimset(@ga);

options =
gaoptimset(options,'PlotFcn',{@gaplotbestf,@gaplotstopping,@gaplotdistance,@gaplotscores,@gaplotselection,@gaplotexpectation,@gaplotscorediversity},'Display','diagnose',

'MutationFcn',@mutationadaptfeasible,'Tolcon',

1e-39,'PopulationSize',800,'Generations',70);

[x, fval] = ga(ObjFcn,nvars,A,b,[  ],[  ],LB,UB,ConsFcn,options);
```

Appendix (4): ANN Algorithm

```
v1=40.94;
v2=40.19;
v3=39.72;
v4=36.7;
v5=34.64;
 v6=27.19;
v7=40.43;
v8=35.93;
v9=39.95;
v10=22.01;
v11=34.02;
v12=40.68;
v13=36.49;
v14=39.48;
v15=35.29;
v16=37.34;
v17=36.78;
v18=29.36;
v19=29.17;
v20=28.93;
v21=18.35;
v22=22.22;
v23=27.19;
v24=40.03;
v25=38.56;
```

v26=39;

v27=38;

v28=37;

v29=36;

v30=45;

v31=35;

v32=34;

v33=33;

v34=32;

v35=31;

v36=31;

v37=33;

v38=35;

v39=37;

v40=39;

v41=32;

v42=34;

v43=36;

v44=38;

v45=40;

v46=39;

v47=39;

v48=39;

v49=39;

v50=39;

a1=0.1457;

a2=0.3763;

a3=0.6685;

a4=1.0334;

a5=1.5445;

a6=0.1359;

a7=0.3362;

a8=0.6408;

a9=1.027;

a10=1.5457;

a11=0.1467;

a12=0.3545;

a13=0.6508;

a14=1.0261;

a15=1.5532;

a16=0.1512;

a17=0.3116;

a18=0.6186;

a19=0.7656;

a20=1.412;

a21=0.1531;

a22=0.2458;

a23=0.318;

a24=0.6447;

a25=1.0507;

a26=0.1494;

a27=0.377;

a28=0.6655;

a29=1.0324;

a30=1.5488;

a31=0.1495;

a32=0.3785;

a33=0.6673;

a34=1.0328;

a35=1.5482;

a36=0.1587;

a37=0.3383;

a38=0.6326;

a39=1.0191;

a40=1.5533;

a41=0.1549;

a42=0.3444;

a43=0.6359;

a44=1.024;

a45=1.555;

a46=0.1525;

a47=0.3622;

a48=0.6531;

a49=1.025;

a50=1.5496;

```
v= {[v1, v6, v11, v16, v21, v26, v31, v36, v41, v46;
    v2, v7, v12, v17, v22, v27, v32, v37, v42, v47;
    v3, v8, v13, v18, v23, v28, v33, v38, v43, v48;
    v4, v9, v14, v19, v24, v29, v34, v39, v44, v49;
    v5, v10, v15, v20, v25, v30, v35, v40, v45, v50]};

a= {[a1, a6, a11, a16, a21, a26, a31, a36, a41, a46;
    a2, a7, a12, a17, a22, a27, a32, a37, a42, a47;
    a3, a8, a13, a18, a23, a28, a33, a38, a43, a48;
    a4, a9, a14, a19, a24, a29, a34, a39, a44, a49;
    a5, a10, a15, a20, a25, a30, a35, a40, a45, a50]};

net1= newff(v,a,{10 10},{'tansig' 'tansig' 'purelin'});
view (net1);
rng('default');
net1.trainParam.epochs = 2000;
net1.trainParam.Momentum = 0.9;
net1.trainParam.InitialLearnRate = 1e-5;
net1.trainParam.L2Regularization = 0.09;
net1.trainParam.MiniBatchSize = 5;
net1.trainParam.Iter = 5000;
net1.trainParam.lr_inc = 1.09;
net1.trainParam.lrgdm=0.01;
net1.trainParam.goal=1e-40;
net1.trainParam.min_grad = 1e-30;
net1.trainParam.max_fail=6;
```

```
net1.performParam.regularization = 0.5;
net1.divideParam.trainRatio = 75/100;
net1.divideParam.valRatio = 25/100;
net1.divideParam.testRatio = 25/100;
net1.trainParam.show = 5;
net1.performFcn = 'msereg';
net1.trainParam.mu=1e-50;
net1.trainParam.mu_inc = 1.005;
net1.trainParam.mc = 0.8;
stream = RandStream.getGlobalStream;
reset(stream);
perf = mse(net1, v, a, 'regularization', 0.02);
net1.performFcn
[net1,tr] = traingda(net1,v,a);
y = net1(v);
[r,m,b] = regression(a,y);
plotregression(a,y)
outputs = net1(v);
errors = gsubtract(a,y);
performance = perform(net1,a,y);
figure, ploterrhist(errors);
gensim(net1,1);
```

Appendix (5): Solar Module

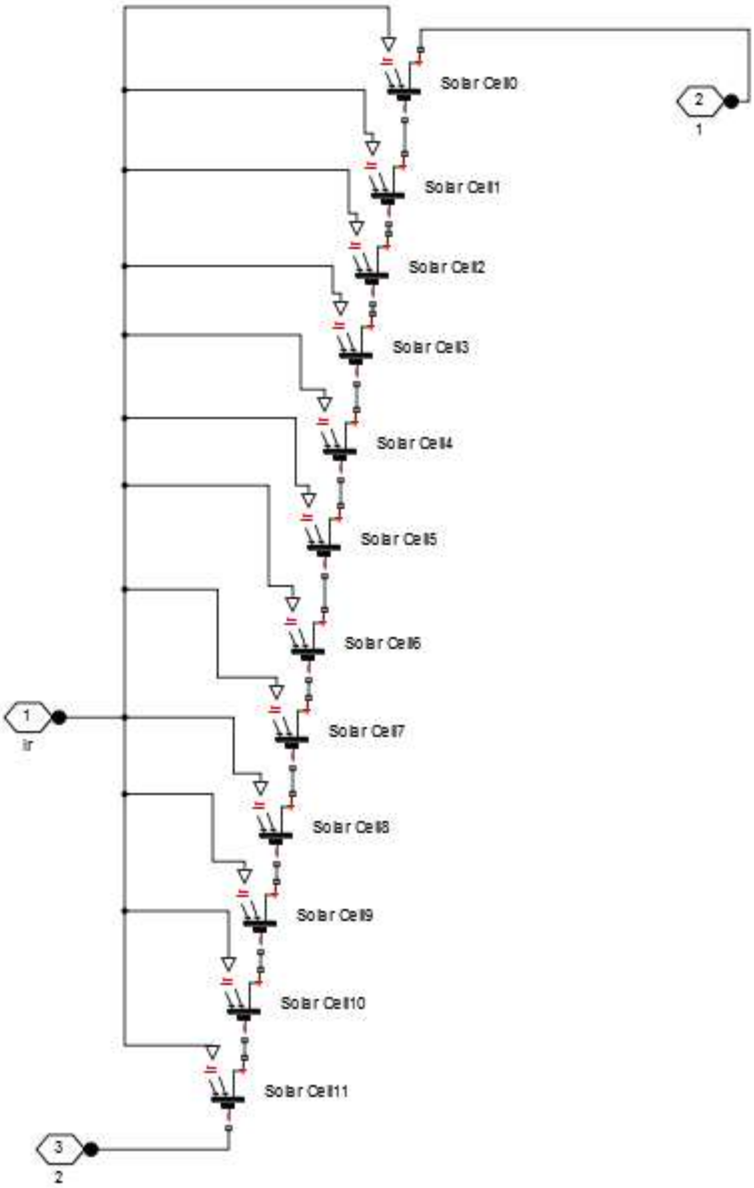

Appendix (6): Pulse Width Modulator

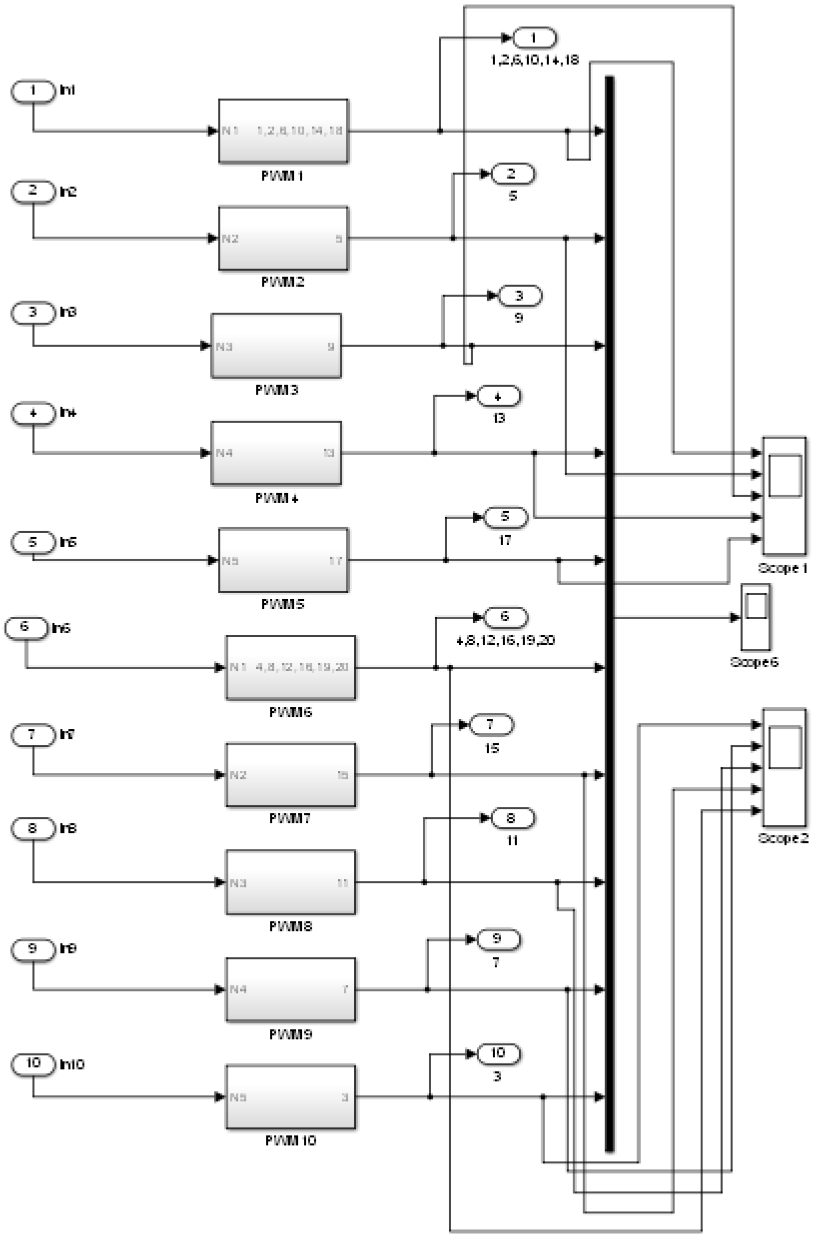

Appendix (7): Eleven-Level Inverter

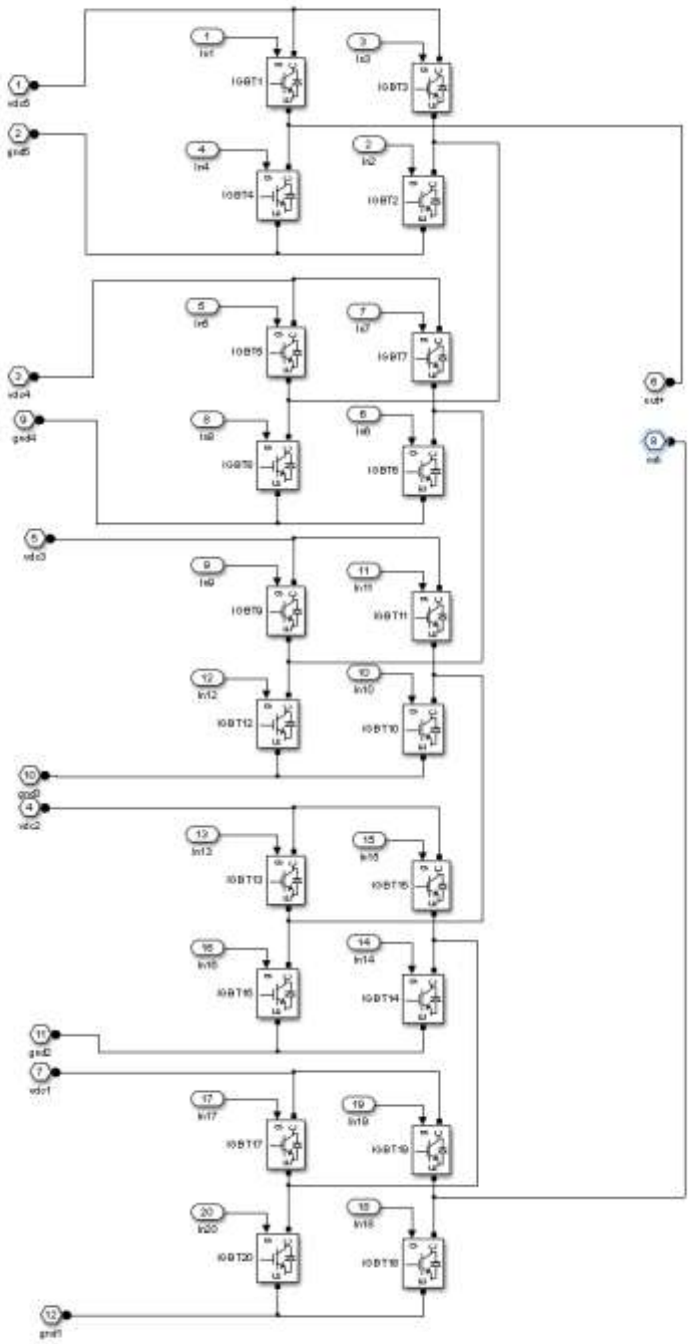

Appendix (8): The SIMULINK Model of Multilevel Inverter (left half)

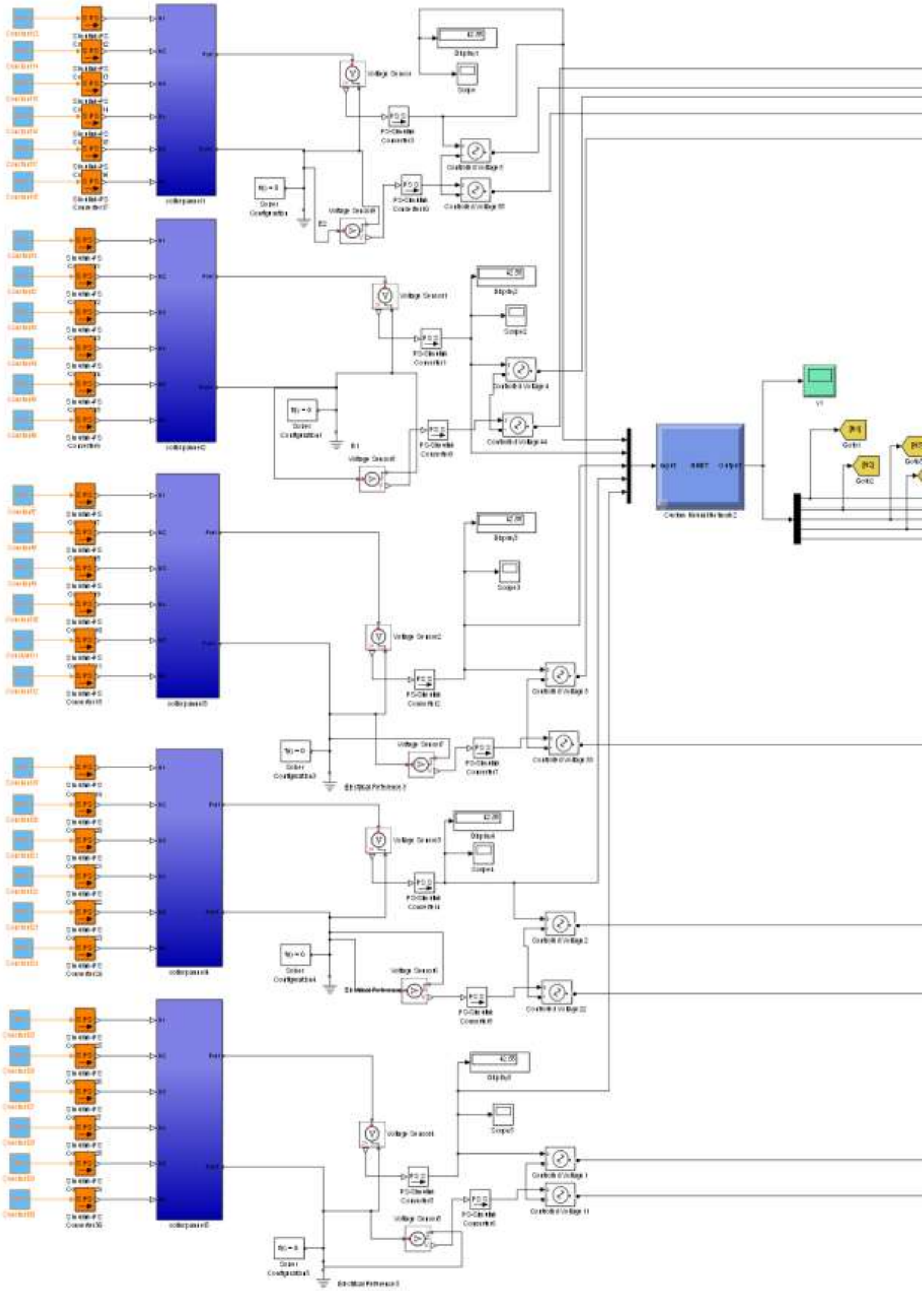

Appendix (8): The SIMULINK Model of Multilevel Inverter (right half)